UCLA
COMPUTATIONAL AND APPLIED MATHEMATICS

On the Real Time Dynamics of Complex Singularities for Burgers' Equation

David Senouf

July 1995

CAM Report 95-33

Department of Mathematics
University of California, Los Angeles
Los Angeles, CA. 90024-1555

ON THE REAL TIME DYNAMICS OF COMPLEX SINGULARITIES FOR BURGERS' EQUATION

DAVID SENOUF*

Dedicated to Sophia de Rosnay

Abstract. Spatial analyticity properties of the solution to Burgers' equation with generic initial data are presented, following the work of Bessis and Fournier [Research Reports in Physics - Nonlinear Physics, Springer Verlag Berlin, Heidelberg 1990, pp. 252-257]. The positive viscosity solution is a meromorphic function with a countable set of conjugate simple poles whose motion on the imaginary axis is governed by an infinite dimensional Calogero type dynamical sytem. The inviscid solution is a three-sheeted Riemann surface with three branch point singularities.

Exact pole locations are found independently of the viscosity at the inviscid shock time t_*. Additionally, the small viscosity behavior of the poles is shown to be a perturbation of the inviscid branch point singularities for $t \leqslant t_*$. A small viscosity asymptotic expansion of the solution uniformly valid in a neighborhood of the inviscid branch points is found in terms of the Pearcey integral.

The solution is computed for small viscosity using pole dynamics, finite differences and asymptotic methods, and numerical agreement is established. The method of pole dynamics consists in finding the evolution of a large set of poles by solving numerically a truncated version of the Calogero dynamical sytem. This system is adjoined with initial data consisting of the exact pole locations at t_*. A Runge-Kutta scheme is used together with a "Multipole" algorithm to deal with the computationally intensive nonlinear interaction of the poles. The solution is reconstructed from the pole positions and the Mittag-Leffler (pole) expansion of the solution. From this procedure, the evolution of the width of the analyticity strip is shown to remain uniformly bounded away from zero, agreeing with the asymptotic predictions.

AMS subject classifications. 35A20, 35A40, 35B40, 35Q53, 41A60

Contents.

* Department of Mathematics, UCLA, Los Angeles, California 90095-1555. Research partially supported by NSF Grant # DMS-9306720.

1. Introduction. In this article we investigate the spatial analyticity properties of a solution to Burgers' equation

$$\frac{\partial u}{\partial t} + u\frac{\partial u}{\partial x} = \nu\frac{\partial^2 u}{\partial x^2}, \qquad x \in \mathbb{R}, t > 0, \nu \geqslant 0, \tag{1.1}$$

where the parameter ν is a viscosity coefficient, and $u = u_\nu(x,t)$ represents the velocity field of a fluid particle at position x in space and time t. Burgers' equation is a model for the statistical theory of turbulence [8, 9] which can be thought of as a simplified one-dimensional scalar analog of the Navier-Stokes equations of fluid dynamics. Although it does not exhibit the complexity of the Navier-Stokes equations, it does illustrate the interaction between a non-linear first order convective term and a second order diffusive one. This feature which is shared with the Navier-Stokes equations may help understand the questions of regularity of so complicated a system. Bardos and Benachour have shown [4] that the loss of analyticity for the incompressible Euler equations in $\mathbb{R}^n$ has to follow a blowup in the vorticity $\omega = \nabla \times u$, in analogy with the blowup of the solution of the inviscid Burgers equation ($\nu = 0$) which is driven by the blowup of the gradient of the solution $\partial u/\partial x$, .

We focus on a particular initial value problem for (1.1) where the initial condition is given by

$$u(x,0) = u_0(x) = 4x^3 - x/t_*, \qquad x \in \mathbb{R}, \tag{1.2}$$

and t_* is a fixed positive parameter. This particular initial value problem was introduced by Bessis and Fournier in [5, 6] following a study by Fournier and Frisch [17]. The inviscid equation is a hyperbolic quasi-linear PDE whose solution develops a cube root singularity at the origin at the time $t = -(\inf_x u_0'(x))^{-1} > 0$, which, for (1.2) equals t_*. This is known to be a generic singularity for the inviscid Burgers equation which is due to the coalescence at the origin ($x = 0$) of two complex conjugate branch points $\pm x_s(t)$ of order two. The cubic initial data is considered to be generic due to the local cube root shape of the shock of the inviscid solution at $t = t_*$ and the associated cube root singularity (for further details, see Appendix A and [6, 10, 17]). When $\nu > 0$, this data generates a (countable) infinite number of complex poles at positive time. Although a higher order polynomial of the form $u_0(x) = 2nx^{2n-1} - x/t_*$ would

also have this property, it would no longer be generic for the inviscid equation (see Appendix A). Another compelling reason for which we choose a cubic polynomial is that its solution can be completely analyzed for both $\nu > 0$ and $\nu = 0$, unlike a higher order polynomial.

In the inviscid case, a classical solution $u \in C^1(\mathbb{R} \times \mathbb{R}_+)$ ceases to exist at $t = t_*$. For $t > t_*$, the solution has three real values within the interval $(-x_s, x_s) \subset \mathbb{R}$, and in the complement $(-x_s, x_s)^c$ it has one real value and two complex values (see Fig. 6.1 and [10]). Thus a natural setting for the analysis of the multi-valuedness of the inviscid Burgers equation is found by extending (for all $t > 0$) the domain of the spatial variable x and the range of the solution u into the complex plane. Bessis and Fournier have shown in [5, 6] that for $\nu = 0$, the analytic structure (topology) of the solution is a three-sheeted Riemann surface with three branch points, one at infinity and two of which come down the imaginary axis as a conjugate pair and coalesce at the origin at the so-called shock time t_* to form a third order branch point. The inviscid shock in the real plane is interpreted as the permutation of the physical Riemann sheets which make up the Riemann surface. More precisely, it appears to be the connecting path between the two sides of the physical Riemann sheet which are seperated by non-physical ones (see [5] for more details).

The positive viscosity solution ($\nu > 0$) is a meromorphic function with a countable set of conjugate pairs of simple poles for all $t > 0$. These poles move towards the origin along the imaginary axis, then turn around after a finite time and start moving away from the origin (see Figs. 6.2 and 6.3). In the same way that the dynamics of the branch points of the inviscid solution help in understanding the formation of a shock in the real (physical) plane, we intend to illustrate the preservation of regularity of the viscous solution by further analyzing the dynamics of the simple poles. In turn, this will shed some light on the interaction between the non-linear convective term and the diffusive one present in the (viscous) Burgers equation. Furthermore, we clarify the limiting process which describes the vanishing viscosity limit by focusing on the small ν asymptotic behavior of the poles. As $\nu \to 0^+$, the poles condense on the imaginary axis, yielding an asymptotic pole density. The inviscid limit can be recovered by introducing an integral representation of the Mittag-Leffler expansion which involves this density. These results are presented in [26]. It should be noted that the analysis of a meromorphic solution to Burgers' equation was first described by Frisch and Morf in [18, section IV]. Recent work has also been done on complex time and space analysis of Burgers' equation with a periodic initial data by Kimura [22].

The structure of this article is as follows: For $\nu > 0$, the solution is explicitly given by the Cole-Hopf transform. From a careful analysis of the Cole-Hopf variable, the solution is expressed in terms of its polar singularities by means of a Mittag-Leffler (pole) expansion. A Calogero-type infinite dimensional dynamical system which governs the time evolution of the poles is found by replacing the pole expansion of the solution into the PDE. This system represents compatibility conditions for the existence of such a pole expansion. From the integral representation obtained via the Cole-Hopf analysis, by means of the saddle point method, we derive an asymptotic formula for the solution $u_\nu(x,t)$ for small ν. However, for any $t \geqslant t_*$, there is a degeneracy in the asymptotic formula at the caustic $x = \pm x_s(t)$ where two saddle points coalesce; thus we derive both the regular saddle point analysis within and outside the caustic, and a uniformly valid expansion via Pearcey's integral which correctly describes the transition between the two regions. The asymptotic behavior of the solution at the

caustic $u_\nu(x_s,t)$ is obtained from the Pearcey representation. As expected, it is shown to match the behavior obtained from the classical saddle point analysis.

For small $\nu > 0$ and $0 < t \leqslant t_*$, we show that the poles are a perturbation of the inviscid branch point singularities of the form $\beta_k(t,\nu) = |x_s(t)| + \mathcal{O}\left((k\nu)^{3/4}\right)$. For $t > t_*$, their asymptotic behavior no longer depends on the inviscid branch point singularities and it is given by $\beta_k(t,\nu) = \mathcal{O}\left((k\nu)^{3/4}\right)$. The actual location of the poles in the non-zero viscosity case has not been described. Thus, we attempt to analyze their time evolution more explicitly by solving numerically a truncated version of the Calogero ODE system. The "initial data" which is adjoined to this truncated system is generated by asymptotic and numerical approximations of the poles at t_*. In [25], the asymptotic expansion of a related Fourier integral is determined by the method of steepest descents which allows for a highly accurate analysis of the pole locations at $t = t_*$, independently of the size of the viscosity. A Runge-Kutta-Fehlberg 4-5 time marching scheme is used in combination with the "Multipole" algorithm designed by Greengard and Rokhlin [19]. This Multipole algorithm reduces the computational complexity of the nonlinear interaction of the poles in the Calogero ODE system from $\mathcal{O}(N^2)$ to $\mathcal{O}(N \log N)$ particles (poles), thereby allowing us to carry out very large simulations with up to $N = 50,000$ poles. The analytical solution to a two-pair pole dynamics is obtained and serves as a test case for the Multipole simulation. The time evolution of the width of the strip of analyticity of the viscous solution is governed by the pole closest to the real axis which can be tracked numerically according to this method. The poles are fixed to the imaginary axis and move towards the origin until a time $t = t_u$; time at which they turn around and move away from the origin. This turn around time t_u occurs before t_* for $\nu \lessapprox .01$, and after t_* for $\nu \gtrapprox .01$ During this process, the poles never reach the real axis, thereby preserving the uniform analyticity of the solution (in agreement with the results of Sulem *et altri* in [29]). It is also observed that t_u increases with decreasing ν, in accordance with the fact that the time at which the solution starts decaying increases with decreasing ν. Additionally, one can use the pole dynamics to compute the solution via the pole expansion and the pole positions at various times. These predictions are compared to those obtained independently from the saddle point analysis and from finite difference approximations. The difference scheme we use is the method of lines consisting of the same Runge-Kutta-Fehlberg 4-5 scheme in time combined with central differencing in space.

2. Integral representation, pole expansion and pole dynamics for $\nu > 0$.

2.1. Cole-Hopf solution and Mittag-Leffler expansion. For $\nu, t > 0$, the Cole-Hopf solution to (1.1) can be represented by a Mittag-Leffler expansion as follows:

THEOREM 2.1. *Let $\nu, t > 0$, then*

$$u_\nu(x,t) = \frac{x}{t} - 2\nu\,\partial_x \log\big(E_\nu(x,t)\big),$$
$$E_\nu(x,t) = \int_{-\infty}^{\infty} \exp\left\{\frac{1}{2\nu}\left(\frac{x}{t}y + \alpha y^2 - y^4\right)\right\} dy,$$

where $2\alpha = 1/t_* - 1/t \in \mathbb{R}$. For fixed ν, t, $E_\nu(x,t)$ is an even entire function of x of order $4/3$ with countably many simple zeros which come in pure imaginary opposite

and conjugate pairs. Moreover, $E_\nu(x,t)$ has the infinite product representation

$$E_\nu(x,t) = C_\nu(t)\prod_{n=1}^{\infty}\left(1+\frac{x^2}{\beta_n^2(t,\nu)}\right), \quad \sum_{n=1}^{\infty}\frac{1}{\beta_n} = +\infty, \quad \sum_{n=1}^{\infty}\frac{1}{\beta_n^2} < +\infty,$$
$$C_\nu(t) = \frac{\sqrt{\alpha}}{2}\,e^{\frac{\alpha^2}{16\nu}}\,K_{1/4}\left(\frac{\alpha^2}{16\nu}\right), \quad C_\nu(t_*) = \nu^{1/4}2^{-3/4}\Gamma(1/4),$$

where $K_q(z)$ is the modified Bessel function of the second kind. Thus the solution $u_\nu(x,t)$ has an alternate representation in terms of a Mittag-Leffler (pole) expansion

$$u_\nu(x,t) = \frac{x}{t} - \sum_{n=1}^{\infty}\frac{4\nu x}{x^2+\beta_n^2(t,\nu)},$$

which converges uniformly on compact sets for x away from the poles $a_n = \pm i\beta_n$.

Proof. The solution to system (1.1) is constructed using the Cole-Hopf nonlinear transform $u = -2\nu\,\partial_x\log(\phi_\nu)$ [15, 20] which was first introduced by Forsyth (cf. [16, §207,p. 100]). This nonlinear dependent variable transformation maps Burgers' equation into the diffusion equation for $\phi_\nu(x,t)$ with corresponding initial data $\phi_0(x) = \exp\{-\frac{1}{2\nu}\int_0^x u_0(y)dy\}$. The solution is therefore represented by means of a convolution:

$$\begin{aligned}\phi_\nu(x,t) &= (K_\nu * \phi_o)(x,t)\\ &= (4\pi\nu t)^{-1/2}\int_{-\infty}^{\infty} e^{-\frac{(x-y)^2}{4\nu t}}e^{-\frac{1}{2\nu}\int_0^y u_0(\eta)d\eta}dy = K_\nu(x,t)E_\nu(x,t),\end{aligned}$$

where $K_\nu(x,t) = K(x,\nu t) = (4\pi\nu t)^{-1/2}\exp(-x^2/4\nu t)$ is the fundamental solution of the diffusion equation, and

$$E_\nu(x,t) = \int_{-\infty}^{\infty}\exp\left\{\frac{1}{2\nu}\left(\frac{xy}{t}-\frac{y^2}{2t}-\int_0^y u_0(\eta)d\eta\right)\right\}dy.$$

Since $\partial_x\log(K_\nu(x,t)) = -x/2\nu t$, the solution of the original problem is given by

$$u_\nu(x,t) = \frac{x}{t} - 2\nu\,\partial_x\log(E_\nu(x,t)). \tag{2.1}$$

For $u_0(x) = 4x^3 - x/t_*$, $\nu, t > 0$, we obtain the following solution:

$$E_\nu(x,t) = \int_{-\infty}^{\infty}\exp\left\{\frac{1}{2\nu}\left(\frac{x}{t}y+\alpha y^2-y^4\right)\right\}dy, \qquad \alpha = \frac{t-t_*}{2tt_*}\in\mathbb{R}. \tag{2.2}$$

It is clear that E_ν is an even, real analytic function of x, and therefore satisfies the conjugacy relation $E_\nu(\overline{x},t) = \overline{E_\nu(x,t)}$ (the analyticity of E_ν can be verified using Morera's Theorem). The positive order λ of an entire function $f(z)$ is defined as $\lambda = \limsup_{r\to+\infty}\log\log M(r)/\log r$, where $M(r) = \max_{|z|=r}|f(z)|$. For a fixed time $t > 0$, the order of E_ν is the smallest number $\lambda\in\mathbb{R}_+$ such that $M_\nu(r) = \max_{|x|=r}|E_\nu(x,t)| \leqslant \exp(r^{\lambda+\epsilon})$ for any $\epsilon > 0$ as soon as r is sufficiently large. From the asymptotic behavior of E_ν for $|x| = r\to+\infty$, we find in (4.3) that $M_\nu(r) = \mathcal{O}(r^{1/3}\exp(-\kappa(t)\,r^{4/3}/2\nu))$ where $\kappa(t)/2\nu$ is the "type" of the entire function E_ν. Thus it is clear that its order is $\lambda = 4/3$. It is known that entire functions of fractional order have infinitely many zeros (see [3, 7]), thus E_ν has infinitely many zeros that come in opposite and conjugate pairs.

Since the fractional order of the entire function E_ν is also the exponent of convergence of its zeros a_n (see again [3, 7]), we have

$$\forall \epsilon > 0, \quad \sum_{n=1}^{\infty} \frac{1}{|a_n|^{\lambda+\epsilon}} < +\infty. \tag{2.3}$$

Using a Hadamard decomposition, we construct the solution u_ν by factorization of the zeros of E_ν. The canonical infinite product expansion of E_ν is (see [3])

$$E_\nu(x,t) = \mathcal{C} x^m e^{g(x)} \prod_{n=1}^{\infty} \left(1 - \frac{x}{a_n}\right) e^{x/a_n + \frac{1}{2}(x/a_n)^2 + \cdots + \frac{1}{p}(x/a_n)^p},$$

where $g(x)$ is a polynomial of degree q. The integer $h = \max(p,q)$ which is called the genus of the product representation of the entire function E_ν satisfies the bound $h \leqslant \lambda \leqslant h+1 \Rightarrow h = 1 \Rightarrow p, q \leqslant 1$. Moreover since E_ν is an even function of x, we must have $q = \deg g(x) = 0$, and therefore $p = 1$ (since $p + 1 > \lambda, p \in \mathbb{N}$). Since $\mathcal{C} = \mathcal{C}_\nu(t) = E_\nu(0,t) \neq 0$ (see (2.6a)), we must also set $m = 0$, so that the canonical product must be of the form

$$E_\nu(x,t) = \mathcal{C}_\nu(t) \prod_{n=1}^{\infty} \left(1 - \frac{x}{a_n}\right) e^{x/a_n}, \quad \sum_{n=1}^{\infty} \frac{1}{|a_n|} = +\infty, \quad \sum_{n=1}^{\infty} \frac{1}{|a_n|^2} < +\infty.$$

Due to the even parity of E_ν, its zeros come in opposite pairs $x = \pm a_n$, thus the product representation reduces to the simple form

$$E_\nu(x,t) = \mathcal{C}_\nu(t) \prod_{n=1}^{\infty} \left(1 - \frac{x^2}{a_n^2}\right).$$

In [24], Pólya showed that functions of the form

$$\int_{-\infty}^{\infty} e^{-at^{4n} + bt^{2n} + iyt} dt \qquad n \geqslant 1, a > 0, b \in \mathbb{R}, \tag{2.4}$$

have only real zeros. Using this property it is straightforward that the zeros of E_ν come in pure imaginary conjugate pairs; thus we let $a_n = i\beta_n$, $\beta_n > 0$ and obtain an infinite product expansion of E_ν valid for all $t, \nu > 0$:

$$E_\nu(x,t) = \mathcal{C}_\nu(t) \prod_{n=1}^{\infty} \left(1 + \frac{x^2}{\beta_n^2(t,\nu)}\right), \quad \sum_{n=1}^{\infty} \frac{1}{\beta_n} = +\infty, \quad \sum_{n=1}^{\infty} \frac{1}{\beta_n^2} < +\infty, \tag{2.5}$$

where $\mathcal{C}_\nu(t)$ is a constant depending on t which can be found explicitly: Let $K_q(z)$ be the modified Bessel function of the second kind, then

$$\mathcal{C}_\nu(t) = E_\nu(0,t) = \int_{-\infty}^{\infty} e^{(\alpha y^2 - y^4)/2\nu}\, dy = \frac{\sqrt{\alpha}}{2} e^{\frac{\alpha^2}{16\nu}} K_{1/4}\left(\frac{\alpha^2}{16\nu}\right), \tag{2.6a}$$

$$\mathcal{C}_\nu(t_*) = E_\nu(0,t_*) = \int_{-\infty}^{\infty} e^{-y^4/2\nu}\, dy = \nu^{1/4} 2^{-3/4} \Gamma(1/4), \tag{2.6b}$$

with $K_{1/4}(z) = \mathcal{O}(z^{-1/4})$ as $z \to 0$. After logarithmic differentiation of E_ν, using (2.1) and (2.5), the spatially singular part of the solution being the ratio of two entire

functions is meromorphic. Thus we obtain a Mittag-Leffler expansion of the solution which we refer to as the (infinite) pole expansion:

$$u_\nu(x,t) = \frac{x}{t} - \sum_{n=1}^{\infty} \frac{4\nu x}{x^2 + \beta_n^2(t,\nu)}. \tag{2.7}$$

Since $\sum_n \beta_n^{-2} < \infty$, for any fixed $t, \nu > 0$, the series defining u_ν in (2.7) converges absolutely and uniformly on any strip $0 < \beta_k < \delta_k \leqslant |\Im x| \leqslant \delta_{k+1} < \beta_{k+1}$, $k \in \mathbb{N}^* = \mathbb{N}\backslash\{0\}$. Therefore u_ν is analytic in the strip $|\Im x| < \beta_1$ where $i\beta_1$ is the first ordered pole on the imaginary axis. From (2.7), u_ν conserves the odd parity of the initial data as expected from the PDE: $u_\nu(-x,t) = -u_\nu(x,t)$. In order for this pole expansion to make sense, the behavior of the spatially singular part of the expansion should be unbounded as $t \to 0^+$ in order to balance with the term x/t. □.

2.1.1. Observation on $E_\nu(x,t)$. Let $'$ denote $\partial/\partial x$ and $E(x) = E_\nu(x,t)$, then for fixed $\nu, t > 0$, $E_\nu(x,t)$ satisfies a third order linear homogeneous ODE in x given by

PROPERTY 2.2.

$$E''' - \frac{\alpha}{8\nu^2 t^2} E' - \frac{x}{32\nu^3 t^4} E = 0.$$

Let $\lambda_\nu(x,t)$ be the roots of the corresponding characteristic polynomial, and let $U(x,t)$ be the spatially singular part of the solution to the inviscid system (6.1), then

$$\lambda_\nu(x,t) = U(x,t)/(2\nu t).$$

Proof. One can differentiate under the integral sign arbitrarily many times due to the factor $\exp(-y^4/2\nu)$ which preserves the convergence of the integrals

$$E^{(k)}(x) = \partial_x^k E(x) = \int_{-\infty}^{\infty} \left(\frac{y}{2\nu t}\right)^k e^{w(y,x)/2\nu} dy, \quad w(y,x) = xy/t + \alpha y^2 - y^4.$$

Since

$$0 = \int_{-\infty}^{\infty} \partial_y e^{w(y,x)/2\nu}\, dy = \int_{-\infty}^{\infty} \frac{1}{2\nu} \left(\frac{x}{t} + 2\alpha y - 4y^3\right) e^{w(y,x)/2\nu}\, dy,$$

we have

$$E''' - \frac{\alpha}{8\nu^2 t^2} E' - \frac{x}{32\nu^3 t^4} E = 0. \tag{2.8}$$

Expressing (2.8) as a first order system , we find

$$\mathcal{E}' = \begin{pmatrix} 0 & 1 & 0 \\ 0 & 0 & 1 \\ \frac{x}{32\nu^3 t^4} & \frac{\alpha}{8\nu^2 t^2} & 0 \end{pmatrix} \mathcal{E} = \mathcal{M}\,\mathcal{E}.$$

where $\mathcal{E} = (E, E', E'')^T$. The eigenvalues $\lambda = \lambda_\nu(x,t)$ of the matrix $\mathcal{M}$ given by the equation $0 = \det(\mathcal{M} - \lambda\mathcal{I})$ are the roots of the characteristic polynomial

$$\lambda^3 - \frac{\alpha}{8\nu^2 t^2}\lambda - \frac{x}{32\nu^3 t^4} = 0.$$

Let $\lambda_\nu = \tilde{\lambda}/(2\nu t)$, then $\tilde{\lambda}$ satisfies the same cubic equation as $U(x,t)$, namely

$$\tilde{\lambda}^3 - \frac{\alpha}{2}\tilde{\lambda} - \frac{x}{4t} = 0,$$

where $U(x,t)$ is the spatially singular component of the inviscid solution (see (6.5)). Using Cardan's formula (see Appendix B), we find that

$$\tilde{\lambda} = U(x,t) = (8t)^{-1/3}\left\{\sqrt[3]{x - \sqrt{x^2 - x_s^2}} + \sqrt[3]{x + \sqrt{x^2 - x_s^2}}\right\}, \tag{2.9}$$

where $x_s = t\,(2\alpha/3)^{3/2}$ is defined in § 4.2. □.

2.2. Calogero dynamical system for the poles $\beta_n(t,\nu)$. We describe the time evolution of the poles $\beta_n(t,\nu)$ according to an infinite dimensional dynamical system which is found as a compatibility condition for the existence of the pole expansion (2.7). We prove the following:

PROPERTY 2.3. *The imaginary part $\beta_n = \beta_n(t,\nu) : \mathbb{R}_+ \times \mathbb{R}_+ \to \mathbb{R}_+$ of the simple poles $x = \pm i\beta_n$ of $u_\nu(x,t)$ satisfy the Calogero-type infinite dimensional dynamical system*

$$\begin{aligned}\forall n \in \mathbb{N}^*, \quad \dot{\beta}_n &= \frac{\beta_n}{t} + \frac{\nu}{\beta_n} - 4\nu\beta_n \sum_{\substack{l=1\\ l\neq n}}^{\infty} \frac{1}{\beta_l^2 - \beta_n^2} \\ &= \frac{\beta_n}{t} - 2\nu \sum_{\substack{l=-\infty\\ l\neq n,0}}^{\infty} \frac{1}{\beta_l - \beta_n}\end{aligned}$$

Moreover, the variables $\gamma_n(t,\nu) = \beta_n^2(t,\nu)/\nu$ satisfying $\sum_n \gamma_n^{-1} < +\infty$ are solution to the ν-independent infinite system of ODEs

$$\forall n \in \mathbb{N}^*, \quad \frac{\dot{\gamma}_n}{2} = \frac{\gamma_n}{t} + 1 - 4\gamma_n \sum_{\substack{l=1\\ l\neq n}}^{\infty} \frac{1}{\gamma_l - \gamma_n}.$$

Proof. The usual pole expansion that is sought in [1, pp. 203-209] and [11, 14, 18] is of the form

$$u_\nu = \sum_{n=1}^{N} \frac{2\nu}{x - i\beta_n}, \tag{2.10}$$

however as $N \to +\infty$ this series diverges for any fixed x, t, ν. Since we have more information about the exact form of the solution, and $\sum_n \beta_n^{-2} < \infty$ from (2.5), instead of using $u_\nu(x,t) = x/t - \sum_n 2\nu/(x - i\beta_n)$ as in [5], we replace the full Mittag-Leffler/pole expansion $u_\nu(x,t) = x/t - \sum_{n=1}^{\infty} 4\nu x/(x^2 + \beta_n^2(t,\nu))$ found in (2.7) in the PDE $u_t + u\,u_x = \nu\,u_{xx}$. Although we are not in the setting of a finite pole-expansion, as it is formulated in the references mentioned above, we can still follow this process to obtain an ODE which governs the motion of the poles $\beta_n(t,\nu)$ as they evolve with time for $t > 0$. We introduce the following notations:

$$\dot{\beta}_n = \frac{d\beta_n}{dt}, \qquad \sum_n = \sum_{n=1}^{\infty}, \qquad \sum_l = \sum_{l=1}^{\infty}, \qquad \sum_{l\neq n} = \sum_{\substack{l=1\\ l\neq n}}^{\infty}.$$

Combining (1.1) and (2.7) we get

$$-\frac{x}{t^2}+8\nu x\sum_n\frac{\beta_n\dot\beta_n}{(x^2+\beta_n^2)^2}+\left(\frac{x}{t}-4\nu x\sum_n\frac{1}{x^2+\beta_n^2}\right)\cdot\left(\frac{1}{t}-4\nu\sum_n\frac{1}{x^2+\beta_n^2}+8\nu x^2\sum_n\frac{1}{(x^2+\beta_n^2)^2}\right)-\nu\left(24\nu x\sum_n\frac{1}{(x^2+\beta_n^2)^2}-32\nu x^3\sum_n\frac{1}{(x^2+\beta_n^2)^3}\right)=0.$$

After distributing the factors, cancelling the terms $\pm x/t^2$, and regrouping terms together in powers of $(x^2+\beta_n^2)^{-2}$, we divide by $8\nu x$ to obtain

$$\sum_n\beta_n\dot\beta_n(x^2+\beta_n^2)^{-2}-\frac{1}{t}\sum_n(x^2+\beta_n^2)^{-1}+\frac{x^2}{t}\sum_n(x^2+\beta_n^2)^{-2}+2\nu\sum_l\sum_n(x^2+\beta_l^2)^{-1}(x^2+\beta_n^2)^{-1}-3\nu\sum_n(x^2+\beta_n^2)^{-2}-4\nu x^2\left(\sum_l\sum_n(x^2+\beta_l^2)^{-1}(x^2+\beta_n^2)^{-2}-\sum_n(x^2+\beta_n^2)^{-3}\right)=0.$$

Since

$$-\frac{1}{t}\sum_n(x^2+\beta_n^2)^{-1}+\frac{x^2}{t}\sum_n(x^2+\beta_n^2)^{-2}=-\frac{1}{t}\sum_n\beta_n^2(x^2+\beta_n^2)^{-2},$$

we regroup the terms in powers of $(x^2+\beta_n^2)^{-1}$ to get

$$\sum_n\left(\beta_n\dot\beta_n-\frac{\beta_n^2}{t}-\nu\right)\cdot(x^2+\beta_n^2)^{-2}+2\nu\left(\sum_n\sum_l(x^2+\beta_n^2)^{-1}(x^2+\beta_l^2)^{-1}-\sum_n(x^2+\beta_n^2)^{-2}\right)-4\nu x^2\left(\sum_n\sum_l(x^2+\beta_n^2)^{-1}(x^2+\beta_l^2)^{-2}-\sum_n(x^2+\beta_n^2)^{-3}\right)=0. \tag{2.11}$$

Using partial fraction expansion we have for $l\neq n$

$$\frac{1}{(x^2+\beta_n^2)(x^2+\beta_l^2)}=\frac{1}{\beta_n^2-\beta_l^2}\cdot\left(\frac{1}{x^2+\beta_l^2}-\frac{1}{x^2+\beta_n^2}\right) \tag{2.12a}$$

$$\frac{1}{(x^2+\beta_n^2)(x^2+\beta_l^2)^2}=\frac{1}{(\beta_l^2-\beta_n^2)^2}\cdot\left(\frac{1}{x^2+\beta_n^2}-\frac{1}{x^2+\beta_l^2}\right)+\frac{1}{\beta_n^2-\beta_l^2}\cdot\frac{1}{(x^2+\beta_l^2)^2} \tag{2.12b}$$

Since

$$\sum_n\sum_{l\neq n}\frac{1}{(\beta_n^2-\beta_l^2)^2}\cdot\left(\frac{1}{x^2+\beta_n^2}-\frac{1}{x^2+\beta_l^2}\right)=0, \tag{2.13}$$

combining (2.12b) and (2.13), we obtain

$$\sum_n \sum_{l\neq n} \frac{1}{(x^2+\beta_n^2)} \cdot \frac{1}{(x^2+\beta_l^2)^2} = \sum_n \sum_{l\neq n} \frac{1}{\beta_n^2-\beta_l^2} \cdot \frac{1}{(x^2+\beta_l^2)^2} = \sum_n \sum_{l\neq n} \frac{1}{\beta_l^2-\beta_n^2} \cdot \frac{1}{(x^2+\beta_n^2)^2}. \tag{2.14}$$

Since we can interchange l and n in (2.12a), we have

$$\sum_n \sum_{l\neq n} \frac{1}{(x^2+\beta_n^2)} \cdot \frac{1}{(x^2+\beta_l^2)} = 2\sum_n \sum_{l\neq n} \frac{1}{\beta_l^2-\beta_n^2} \cdot \frac{1}{(x^2+\beta_n^2)}. \tag{2.15}$$

We replace (2.14) and (2.15) in (2.11) to get

$$\sum_n \left(\beta_n\dot{\beta}_n - \frac{\beta_n^2}{t} - \nu\right) \cdot \frac{1}{(x^2+\beta_n^2)^2} + 4\nu \sum_n \sum_{l\neq n} \frac{1}{\beta_l^2-\beta_n^2} \cdot \frac{1}{(x^2+\beta_n^2)} - 4\nu x^2 \sum_n \sum_{l\neq n} \frac{1}{\beta_l^2-\beta_n^2} \cdot \frac{1}{(x^2+\beta_n^2)^2} = 0.$$

Replacing $(x^2+\beta_n^2)^{-1}$ by $(x^2+\beta_n^2)/(x^2+\beta_n^2)^2$ in the second summation we get

$$\sum_n \left(\beta_n\dot{\beta}_n - \frac{\beta_n^2}{t} - \nu + 4\nu\beta_n^2 \sum_{l\neq n} \frac{1}{\beta_l^2-\beta_n^2}\right) \cdot \frac{1}{(x^2+\beta_n^2)^2} = 0. \tag{2.16}$$

Since (2.16) has to be satisfied for all $x \in \mathbb{C}\backslash \cup_{n\in\mathbb{N}^*}\{x = i\beta_n\}$, it yields the desired system of ordinary differential equations governing the time evolution of the poles β_n:

$$\forall n \in \mathbb{N}^*, \quad \dot{\beta}_n = \frac{\beta_n}{t} + \frac{\nu}{\beta_n} - 4\nu\beta_n \sum_{l\neq n} \frac{1}{\beta_l^2-\beta_n^2}. \tag{2.17}$$

This system may be re-written as

$$\forall n \in \mathbb{N}^*, \quad \dot{\beta}_n = \frac{\beta_n}{t} - 2\nu \sum_{\substack{l=-\infty \\ l\neq n,0}}^{\infty} \frac{1}{\beta_l-\beta_n} \tag{2.18}$$

where the sum must be understood as a symmetric "principal value" sum. This system may be thought of as a set of compatibility conditions that acompany the pole expansion. Introducing the variable $\gamma_n(t,\nu) = \beta_n^2(t,\nu)/\nu$, we have $\sum_n \gamma_n^{-1} < +\infty$, and system (2.17) becomes independent of ν:

$$\forall n \in \mathbb{N}^*, \quad \frac{\dot{\gamma}_n}{2} = \frac{\gamma_n}{t} + 1 - 4\gamma_n \sum_{l\neq n} \frac{1}{\gamma_l-\gamma_n}. \tag{2.19}$$

3. Asymptotic analysis of $u_\nu(x,t)$ as $\nu \to 0^+$, $t > t_*$. When $\nu \to 0^+$, we evaluate the asymptotic behavior of E_ν using the saddle point method. The caustic $x = x_s(t)$ correponds to the envelope of the characteristics of the inviscid Burgers solution, and is also determined by the system of equations

$$\begin{cases} 0 = w_z(z,x) = x/t + 2\alpha z - 4z^3 \\ 0 = w_{zz}(z,x) = 2\alpha - 12z^2 \end{cases} \tag{3.1}$$

where $w(z,x)$ is the phase function of the integrand in the definition of $E_\nu(x,t)$. This system represents the conditions for the phase function w to have saddle points of multiplicity two, thereby yielding a curve in the (x,t) plane on which two saddle points of multiplicity one coalesce into a saddle point of multiplicity two. From the second equation in (3.1), we find $z_{caustic}(t) = \pm\sqrt{\alpha/6}$, and from the first,

$$x = x_{caustic} = t(4z_{caustic}(t)^3 - 2\alpha z_{caustic}(t)) = \mp t\left(\frac{2\alpha}{3}\right)^{3/2} = \mp x_s(t), \tag{3.2}$$

where $x_s(t) = i(3t_*)^{-3/2}(t_* - t)^{3/2}t^{-1/2}$ is the second order branch point of the inviscid solution described in § 6. We find that all three saddle points may be relevant within the caustic $|x| < |x_s(t)| - \delta/2$, where $\delta > 0$. For a discussion on such caustics, cf. [21, 23]. When $t > t_*$, $x \in (-\infty, -x_s(t) - \delta/2) \cup (x_s(t) + \delta/2, \infty)$, $\nu \to 0^+$, the same analysis holds and one recovers the characteristic solution outside the caustic consisting of only one relevant saddle point. The transition from within the caustic to outside is not uniform as the asymptotic behavior at the caustic $x = \pm x_s(t)$ is degenerate (2 saddle points have coalesced). The transitionary regime from one relevant saddle point to two at and around the caustic is therefore described by means of the Pearcey integral which allows for a uniformly valid description.

3.1. Inner expansion: $x \in (-x_s(t) + \delta/2, x_s(t) - \delta/2)$, $\delta > 0$, $t > t_*$. In the analysis that follows, we are only concerned with the dominant behavior of E_ν, thus we only retain the first term:

$$E_\nu(x,t) = \sum_{s=0,1,2} \sqrt{\frac{-4\pi\nu}{w_{zz}(z_s,x)}} \exp\left(\frac{w(z_s,x)}{2\nu}\right)\Big(1 + \mathcal{O}(\nu)\Big), \tag{3.3}$$

as $\nu \to 0^+$, with

$$w_z(z_s(x,t),x) = 0, \quad w_{zz}(z_s(x,t),x) = 2\alpha - 12z_s^2. \tag{3.4}$$

Since

$$0 = \frac{z_s}{4}w_z(z_s,x) = \frac{xz_s}{4t} + \frac{\alpha}{2}z_s^2 - z_s^4,$$

we have that

$$w(z_s(x,t),x) = \frac{x}{t}z_s + \alpha z_s^2 - z_s^4 = \frac{3}{4}\frac{x}{t}z_s + \frac{\alpha}{2}z_s^2. \tag{3.5}$$

The values of the saddle points $z_s = z_s(x,t)$ of (3.3) are determined by the three roots of the first equation in system (3.1), i.e. the first equation of (3.4). They are specifically

$$\begin{cases} z_0 = \omega\mathcal{A} + \omega^2\mathcal{B} \\ z_1 = \omega^2\mathcal{A} + \omega\mathcal{B} \\ z_2 = \mathcal{A} + \mathcal{B} \end{cases} \tag{3.6}$$

with $w = e^{2\pi i/3}$ is a cube root of unity, and

$$\begin{cases} \mathcal{A}(x,t) = (8t)^{-1/3} \cdot \sqrt[3]{x + \sqrt{x^2 - x_s^2}} \\ \mathcal{B}(x,t) = (8t)^{-1/3} \cdot \sqrt[3]{x - \sqrt{x^2 - x_s^2}} \end{cases} \tag{3.7}$$

Note that all three saddle points are real when $x, x_s \in \mathbb{R}$ and the discriminant $\Delta = x^2 - x_s^2 < 0$, that is $|x| < |x_s(t)|$, and in this case $\mathcal{A} = \overline{\mathcal{B}}$ (see Appendix B). Therefore we have $z_s \in \mathbb{R}$, $w(z_s, x) \in \mathbb{R}$, and $w_{zz}(z_s, x) = 2\alpha - 12z_s^2 \in \mathbb{R}$. Hence all three terms in the summation signs may be relevant. Note however that the expansion derived for E_ν is only valid within $|x| < |x_s|$, and in order to get an expansion uniformly valid across $x = \pm x_s$ one needs to derive a uniform expansion as presented in § 3.3. The dominant behavior of the solution $u_\nu(x,t)$ is found from the Cole-Hopf representation, so that within the caustic $|x| < |x_s| - \delta/2$ we have

$$\begin{aligned}\frac{U_\nu(x,t)}{t} &= 2\nu\,\partial_x \log(E_\nu(x,t)) \\ &= 2\nu\,\partial_x \log\left(\sum_{s=0,1,2}\sqrt{\frac{-4\pi\nu}{w_{zz}(z_s,x)}}e^{\frac{w(z_s,x)}{2\nu}}(1+\mathcal{O}(\nu))\right) \\ &= 2\nu\,\frac{\sum_{s=0,1,2}\partial_x\left(\sqrt{\frac{-4\pi\nu}{w_{zz}(z_s,x)}}e^{\frac{w(z_s,x)}{2\nu}}\right)}{\sum_{s=0,1,2}\sqrt{\frac{-4\pi\nu}{w_{zz}(z_s,x)}}e^{\frac{w(z_s,x)}{2\nu}}} + \mathcal{O}(\nu^2).\end{aligned}$$

Since $w(z_s, x) \in \mathbb{R}$ and $\nu > 0$, and since

$$\frac{\partial w}{\partial x}(z_s, x) = \frac{z_s}{t}, \tag{3.8}$$

we find

$$U_\nu(x,t) = \frac{\sum_{s=0,1,2} z_s \cdot e^{\frac{w(z_s,x)}{2\nu}}/\sqrt{w_{zz}(z_s,x)}}{\sum_{s=0,1,2} e^{\frac{w(z_s,x)}{2\nu}}/\sqrt{w_{zz}(z_s,x)}} + \mathcal{O}(\nu). \tag{3.9}$$

The x-differentiation of the asymptotic formula of $E_\nu(x,t)$ is justified due to the analytic dependency in x. Often one of the three saddle points is such that $w(z_s, x) < 0$ and as such its contribution is exponentially smaller than that of the other two. In terms of numerical computation that are carried out in § 5, leaving this term in (3.1) does not affect the value of u_ν. Thus we can simplify the expression (3.9) to a two-term asymptotic expansion which is similar to the one in [32, §4.2]. Clearly the further we are away from the caustic, the more dominant one of the saddle points becomes. However, since there is a point where the dominance of one over the other changes (i.e. where they are equally relevant), we must leave both in the asymptotic formula:

PROPERTY 3.1. *As $\nu \to 0^+$ for $x \in (-x_s(t) + \delta/2, x_s(t) - \delta/2)$, $\delta > 0$, $t > t_*$, the solution to Burgers' equation is given by*

$$u_\nu(x,t) = \frac{x}{t} - \frac{U_\nu(x,t)}{t}, \quad U_\nu(x,t) = \frac{\sum_{\{s:w(z_s,x)>0\}} z_s \cdot e^{\frac{w(z_s,x)}{2\nu}}/\sqrt{w_{zz}(z_s,x)}}{\sum_{\{s:w(z_s,x)>0\}} e^{\frac{w(z_s,x)}{2\nu}}/\sqrt{w_{zz}(z_s,x)}} + \mathcal{O}(\nu).$$

3.2. Outer expansion: $x \in (-x_s(t) - \delta/2, x_s(t) + \delta/2)^c$, $\delta > 0$, $t > t_*$. The inviscid limit is found in a straightforward manner in this case: only one saddle point is relevant, so that the asymptotic limit derived in § 3.1 reduces to

$$U_\nu(x,t) = U(x,t) + \mathcal{O}(\nu) \qquad \text{as } \nu \to 0^+,$$

where $U(x,t) = z_{s*}(x,t)$ is the spatially singular part of the inviscid solution (see § 6). The particular saddle point z_{s*} that is chosen at every x is the one for which $w(z_{s*},x) = \max_{s=0,1,2} w(z_s,x)$. Hence we have outside of the caustic

PROPERTY 3.2. *As $\nu \to 0^+$ for $x \in (-x_s(t)-\delta/2, x_s(t)+\delta/2)^c$, $\delta > 0$, $t > t_*$, the solution to Burgers' equation is given by*

$$u_\nu(x,t) = \frac{x}{t} - \frac{U_\nu(x,t)}{t} = \frac{x}{t} - \frac{U(x,t)}{t} + \mathcal{O}(\nu),$$
$$U(x,t) = z_{s*}(x,t), \quad z_{s*} : w(z_{s*},x) = \max_{s=0,1,2} w(z_s,x).$$

where $U(x,t)$ is the Lagrangian characteristic variable of the inviscid solution.

3.3. Uniform asymptotic expansion in a neighborhood of the caustics $x = \pm x_s(t)$ via Pearcey's integral. Following the notation of Kaminski in [21], we introduce the Pearcey integral from which one can derive a uniform asymptotic expansion with two coalescing saddle points: Let

$$P(X,Y) = \int_{-\infty}^{+\infty} e^{i\left(v^4/4 + Xv^2/2 + Yv\right)}\, dv \tag{3.10}$$

denote the Pearcey integral. Introducing the change of variable $y \to (-i\nu/2)^{1/4} v$ and deforming the path of integration back to the real axis using Jordan's lemma, we can express $E_\nu(x,t)$ as

$$\begin{aligned} E_\nu(x,t) &= \int_{-\infty}^{+\infty} \exp\left\{\frac{-1}{2\nu}\left(y^4 - \alpha y^2 - \frac{x}{t}y\right)\right\} dy \\ &= \left(\frac{-i\nu}{2}\right)^{1/4} \int_{-\infty}^{+\infty} \exp\left\{i\left(\frac{v^4}{4} - \frac{\alpha e^{i\frac{\pi}{4}}}{\sqrt{2\nu}}\frac{v^2}{2} - \frac{x e^{i\frac{3\pi}{8}}}{2t}\left(\frac{1}{2\nu^3}\right)^{1/4} v\right)\right\} dv \\ &= \left(\frac{-i\nu}{2}\right)^{1/4} P\left(X = -\frac{\alpha e^{i\frac{\pi}{4}}}{\sqrt{2\nu}}, Y = -\frac{x e^{i\frac{3\pi}{8}}}{2t}\left(\frac{1}{2\nu^3}\right)^{1/4}\right). \end{aligned} \tag{3.11}$$

Clearly a small ν asymptotic of E_ν is equivalent to a combined asymptotic expansion of the Pearcey integral as $|X|, |Y| \to +\infty$. The caustic of $P(X,Y)$ and the corresponding caustic of $E_\nu(x,t)$ is given by

$$Y = \frac{2}{\sqrt{27}} X^{3/2} \Longleftrightarrow x = \pm x_s(t). \tag{3.12}$$

Hence the uniform asymptotic behavior of E_ν in a neighborhood of the caustic is found from the one of $P(-X, (2/\sqrt{27} - \tau)X^{3/2})$ as $X \to +\infty$, where $\tau = 0$ at the caustic, and $\tau \neq 0$ away from it (see [21]). This amounts to a uniformly valid expansion in the interval $|x + x_s(t)| \leqslant |\delta(\tau;t)|$ where $\delta(\tau) = \delta(\tau;t) = \sqrt{27} x_s(t) \cdot \tau/2 \in \mathbb{R}$. This expansion is also valid outside of this interval, however the region of interest is a close neighborhood of the caustic. Indeed one only needs to use the asymptotic expansion of the Airy function and its derivative to find the results obtained in § 3.1 and § 3.2. From (3.11) we have that

$$\begin{aligned} U_\nu(x,t) &= t \cdot 2\nu\, \partial_x \log(E_\nu(x,t)) \\ &= t \cdot 2\nu\, \partial_x \log\left[P\left(X(\nu;t) = \frac{-\alpha e^{i\pi/4}}{\sqrt{2\nu}}, Y(\nu;x,t) = \frac{-x e^{i3\pi/8}}{2t}\left(\frac{1}{2\nu^3}\right)^{1/4}\right)\right]. \end{aligned}$$

Let

$$X = X(\nu;t), \qquad Y = Y(\nu;t) = Y(\nu; x = -x_s(t) + \delta(\tau;t), t),$$

where $\delta(\tau;t) \to 0^+$ as $\tau \to 0^+$, so that

$$\begin{aligned} U_\nu\Big(x = -x_s(t) + \delta(\tau;t), t\Big) &= t \cdot 2\nu\, \partial_x \log\left(P\left(X(\nu;t), Y(\nu; x = -x_s(t) + \delta(\tau;t), t)\right)\right) \\ &= t \cdot 2\nu\, \partial_\tau \log\left(P\left(-X, (2/\sqrt{27} - \tau)X^{3/2}\right)\right) \Big/ \frac{\partial \delta}{\partial \tau}\,. \end{aligned}$$

Let $P(\tau) = P\left(-X, (2/\sqrt{27} - \tau)X^{3/2}\right)$, then since $\partial\delta/\partial\tau = \sqrt{27}x_s(t)/2$, we have

$$t^{-1}U_\nu\Big(x = -x_s(t) + \delta(\tau;t), t\Big) = \frac{4\nu}{\sqrt{27}x_s(t)} \frac{P_\tau(\tau)}{P(\tau)}.$$

The following Property is found in [21]:

PROPERTY 3.3. *The uniform asymptotic expansion of* $P(-X, (\frac{2}{\sqrt{27}} - \tau)X^{3/2})$ *as* $X \to +\infty$ *in a neighborhood of* $\tau = 0$ *is given by*

$$\begin{aligned} P\left(-X, \left(\frac{2}{\sqrt{27}} - \tau\right)X^{3/2}\right) = \Bigg[e^{iX^2[f(v_2)+f(v_3)]/2} \cdot \Bigg\{p_0(\tau) \cdot \frac{2\pi}{X^{1/6}} \cdot Ai(-X^{4/3}\zeta(\tau)) \\ + q_0(\tau)\frac{2\pi}{iX^{5/6}} Ai'(-X^{4/3}\zeta(\tau))\Bigg\} + e^{iX^2 f(v_1)}\left(\frac{\pi}{3v_1^2 - 1}\right)^{1/2} \frac{1+i}{X^{1/2}}\Bigg] \cdot \left(1 + \mathcal{O}\left(\frac{1}{X^2}\right)\right), \end{aligned}$$

with

$$p_0(\tau) = 3^{-1/6}(1 + \mathcal{O}(\tau)), \quad q_0(\tau) = -\frac{3^{-5/6}}{2}(1 + \mathcal{O}(\tau)), \quad \zeta(\tau) = 3^{-1/6}\tau(1 + \mathcal{O}(\tau)),$$

and

$$f(v) = f(v;\tau) = \frac{v^4}{4} - \frac{v^2}{2} + \left(\frac{2}{\sqrt{27}} - \tau\right)v,$$

and the $v_i, i = 1,2,3$ *are the saddle points of* $f(v;\tau)$ *determined by the equation* $f_v(v_i;\tau) = 0$, *so that* $f(v_i;\tau) = -v_i^2/4 + (2/\sqrt{27} - \tau)3v_i/4$. *The* v_i*'s are specifically*

$$v_1(\tau) = -\frac{2}{\sqrt{3}}\sin\left(\frac{\pi}{3} + \phi(\tau)\right), \quad v_2(\tau) = \frac{2}{\sqrt{3}}\sin(\phi(\tau)), \quad v_3(\tau) = \frac{2}{\sqrt{3}}\sin\left(\frac{\pi}{3} - \phi(\tau)\right),$$

where

$$\phi = \phi(\tau) = \frac{1}{3}\arcsin\left(1 - \tau\sqrt{27}/2\right), \quad \tau \in \mathbb{R}, \quad |\phi| \leqslant \frac{\pi}{6}.$$

In order to derive the uniform asymptotic expansion of the derivative P_τ, on can differentiate termwise the expression in Property 3.3 due to the analytic dependency of $P(X,Y)$ in both its arguments X, Y (see [21] and [31, p. 52]). Therefore since

$$X = \frac{-\alpha e^{i\pi/4}}{\sqrt{2\nu}} \Rightarrow \frac{iX^2}{2} = -\frac{\alpha^2}{4\nu} \Rightarrow X^{-2} = \mathcal{O}(\nu),$$

and

$$\frac{\partial f}{\partial \tau}(v_i;\tau) = -v_i, \quad \frac{\partial f}{\partial v}(v_i;\tau) = 0 \quad \Rightarrow \quad \frac{df}{d\tau}(v_i(\tau);\tau) = -v_i(\tau),$$

and using the fact that $2\alpha/3 = (x_s/t)^{2/3}$, we find that

PROPERTY 3.4. *The uniform asymptotic expansion as* $\nu \to 0^+$ *of* $U_\nu\big(x = -x_s(t) + \delta(\tau;t), t\big)$ *in a neighborhood of the caustic* $x = -x_s(t)$ *is*

$$\begin{aligned} U_\nu\Big(x = -x_s(t) + \delta(\tau;t), t\Big) = \frac{\sqrt{3}}{2}\left(\frac{x_s(t)}{t}\right)^{1/3} \times \Bigg[[v_2 + v_3] e^{-\frac{\alpha^2}{4\nu}[f(v_2)+f(v_3)]} \\ \times \left\{ p_0(\tau) \cdot \frac{2\pi}{X^{1/6}} \cdot Ai(-X^{4/3}\zeta(\tau)) + q_0(\tau)\frac{2\pi}{iX^{5/6}} Ai'(-X^{4/3}\zeta(\tau)) \right\} \\ + 2v_1\, e^{-\frac{\alpha^2}{4\nu}2f(v_1)} \left(\frac{\pi}{3v_1^2 - 1}\right)^{1/2} \frac{1+i}{X^{1/2}} \Bigg] \\ \Bigg/ \Bigg[e^{-\frac{\alpha^2}{4\nu}[f(v_2)+f(v_3)]} \cdot \left\{ p_0(\tau) \cdot \frac{2\pi}{X^{1/6}} \cdot Ai(-X^{4/3}\zeta(\tau)) + q_0(\tau)\frac{2\pi}{iX^{5/6}} Ai'(-X^{4/3}\zeta(\tau)) \right\} \\ + e^{-\frac{\alpha^2}{4\nu}2f(v_1)} \left(\frac{\pi}{3v_1^2 - 1}\right)^{1/2} \frac{1+i}{X^{1/2}} \Bigg] + \mathcal{O}(\nu) \qquad \text{as } \nu \to 0^+. \end{aligned}$$

3.3.1. Behavior at the caustics $x = \pm x_s(t)$. At the caustic $x = -x_s(t)$, $\tau = 0$, $\phi(0) = \pi/6$, $v_1(0) = -2/\sqrt{3}$, $v_2(0) = v_3(0) = 1/\sqrt{3}$. Moreover $f(v_i;0) = -v_i^2/4 + v_i/2\sqrt{3}$, so that $f(v_2;0) = f(v_3;0) = -2/3$ and $f(v_1;0) = 1/12$. Since $f(v_2;0) < 0$ and $f(v_1;0) > 0$, the dominant term as $\nu \to 0^+$ in both the numerator and denominator of U_ν is obviously the one containing the exponentially increasing factor $\exp(-\frac{\alpha^2}{4\nu}[f(v_2) + f(v_3)])$. Therefore the dominant behavior of $U_\nu(-x_s(t),t)$ reduces to the simple form

$$\begin{aligned} U_\nu(-x_s(t),t) &= \frac{\sqrt{3}}{2}\left(\frac{x_s(t)}{t}\right)^{1/3} \cdot (v_2(0) + v_3(0)) + \mathcal{O}(\nu) \\ &= \left(\frac{x_s(t)}{t}\right)^{1/3} + \mathcal{O}(\nu) \quad \text{as } \nu \to 0^+. \end{aligned}$$

Thus since $u_\nu(x,t) = x/t - U_\nu(x,t)/t$, and from the odd parity of u_ν, it follows that

PROPERTY 3.5. *The asymptotic behavior of the solution* $u_\nu(x,t)$ *as* $\nu \to 0^+$ *at the caustic* $x = \pm x_s(t)$ *for* $t > t_*$ *is*

$$u_\nu(\pm x_s(t),t) = \pm\frac{x_s(t)}{t} \mp \frac{1}{t}\left(\frac{x_s(t)}{t}\right)^{1/3} + \mathcal{O}(\nu).$$

This matches the solution found from a classical saddle point analysis obtained by combining (3.2) and (3.6): when $x = x_s(t)$, both saddle points z_0, z_1 coalesce into $z_s = (x_s(t)/t)^{1/3}$. From the asymptotic formula

$$u_\nu(x,t) = \frac{x}{t} - \frac{z_s(x,t)}{t} + \mathcal{O}(\nu),$$

derived in Section 3.2, Property 3.5 is verified. Note that this expression is valid only for $t \geqslant t_* + \varepsilon$, $\varepsilon > 0$.

4. Pole locations.

4.1. Exact pole location at $t = t_*$. From the integral representation (2.2), a Taylor expansion about $x = 0$ can be obtained when $t = t_*$:

PROPERTY 4.1. *Let*

$$\mathcal{S}_\nu(z) = \nu^{1/4} 2^{-3/4} \sum_{n=0}^{\infty} (-1)^n \frac{\Gamma(\frac{2n+1}{4})}{\Gamma(2n+1)} z^{2n}, \qquad |z| < +\infty,$$

which converges absolutely and uniformly on compact sets for z. Then

$$E_\nu(x, t_*) = \mathcal{S}_\nu\left(\frac{ix}{4t_*}(2\nu)^{-3/4}\right), \qquad |x| < +\infty.$$

Let $x = i\beta$, $\beta \in \mathbb{R}$, $|\beta| < +\infty$, then if we introduce the scaling

$$\beta = \beta(t_*, \nu) = 4t_*(2\nu\mu)^{3/4}, \tag{4.1}$$

we have

$$E_\nu(i\beta, t_*) = \mathcal{S}_\nu\left(\mu^{3/4}\right). \tag{4.2}$$

Following this scaling, we transform the integral representation of $E_\nu(i\beta, t_*)$ to simplify its analysis. At the inviscid shock time t_*,

$$E_\nu(i\beta, t_*) = \int_{-\infty}^{\infty} \exp\left\{\frac{1}{2\nu}\left(\frac{i\beta}{t_*}y - y^4\right)\right\} dy,$$

the change of variable

$$y \to \left(\frac{\beta}{4t_*}\right)^{1/3} z \tag{4.3}$$

introduces the scaling factor (4.1) between the imaginary part β_n of the zeros a_n and the viscosity ν. This allows us to express $E_\nu(i\beta, t_*)$ in terms of a new function $F(\mu)$ which has the advantage that its saddle points are fixed to the unit disc (thereby making the asymptotic analysis simpler):

$$E_\nu(i\beta, t_*) = \left(\frac{\beta}{4t_*}\right)^{1/3} F\left(\frac{1}{2\nu}\left(\frac{\beta}{4t_*}\right)^{4/3}\right), \quad F(\mu) = \int_{-\infty}^{\infty} e^{\mu(4iz - z^4)} dz. \tag{4.4}$$

Once the zeros $\{\mu_k\}_{k=1}^{\infty}$ of $F(\mu)$ are found (independently of ν), the poles $\pm a_k(t_*, \nu) = \pm i\beta_k(t_*, \nu)$ of $u_\nu(x, t_*)$ are given by the relation

$$\beta_k(t_*, \nu) = 4t_*(2\nu\mu_k)^{3/4}, \tag{4.5}$$

which was introduced in (4.1). It is important to see that this relation is valid regardless of whether ν is small or β is large. Thus if we can desbcribe the μ_k's accurately, then the pole locations are known with great precision at t_* (independently of ν). Furthermore the expansion of $E_\nu(i\beta, t_*)$ as $\nu \to 0^+$ or as $\beta \to +\infty$ is determined by that of $F(\mu)$ as $\mu \to +\infty$. The following theorem is proved in [25]:

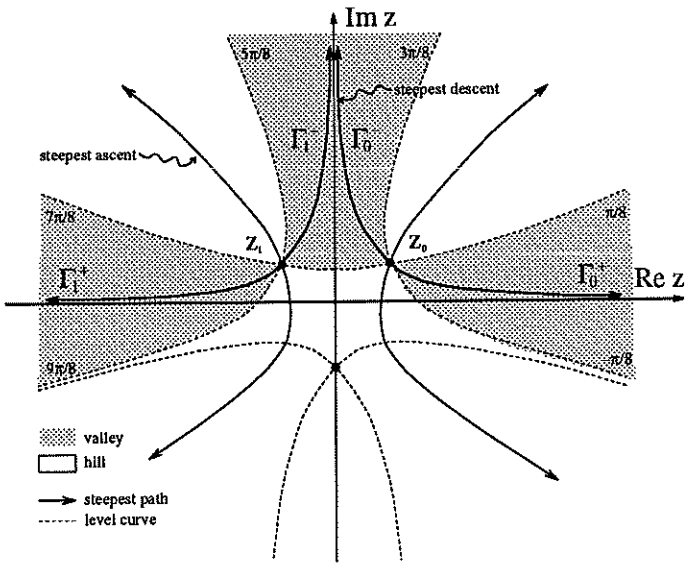

FIG. 4.1. *Hills, valleys, level curves and steepest paths of the saddle points* $z_0 = e^{i\pi/6}$, $z_1 = e^{i5\pi/6}$ *relevant to the expansion of* $F(\mu) = \int_{-\infty}^{\infty} e^{\mu(4iz-z^4)}dz$ *as* $\mu \to +\infty$.

THEOREM 4.2. *The asymptotic expansion of* $F(\mu) = \int_{-\infty}^{\infty} e^{\mu(4iz-z^4)}dz$ *as* $\mu \to +\infty$ *centered about the sector* $|\arg\mu| < \pi/2$ *is*

$$F(\mu) = \sqrt{\frac{2\pi}{3\mu}} e^{-\frac{3}{2}\mu} \left[\cos\left(3\frac{\sqrt{3}}{2}\mu - \frac{\pi}{6}\right) + \mathcal{O}\left(\frac{1}{\mu}\right)\right] \quad \text{as } \mu \to +\infty.$$

Moreover, the k-th ordered positive zero μ_k *of* $F(\mu)$ *is given by (for* $k \geqslant 1$*)*

$$\mu_k^{(0)} = \frac{2\pi}{3\sqrt{3}}(k - 1/3), \qquad \mu_k = \mathcal{G}\left(\mu_k^{(0)}\right) + \mathcal{O}\left(\frac{1}{k^6}\right) \quad \text{as } k \to +\infty,$$
$$\mathcal{G}(\mu) = \mu + \frac{7}{432\mu}\left(1 - \frac{1}{6\mu}\left(1 + \frac{7}{72\mu}\left(1 - \frac{5}{12\mu}\left(1 + \frac{53143}{18900\mu}\right)\right)\right)\right).$$

Additionally to this asymptotic description, the first 9 values of μ_k are computed numerically in [25] and are listed in § 5. The accuracy of this asymptotic approximation is discussed in [25]; the necessity for such high accuracy will be apparent in § 5.

4.2. Asymptotic analysis of the pole locations as $\nu \to 0^+$ for $t \neq t_*$. The saddle point analysis of $E_\nu(i\beta, t)$ as $\nu \to 0^+$ in the case $t \neq t_*$ is very similar to the one that is described in [25]. There are again two equally relevant saddle points which come in a symmetric pair, and the steepest descent paths are very similar to those displayed in Fig. 4.1, except that the saddle points are either closer together or further apart depending on whether $t < t_*$ or $t > t_*$.

Let $w(z, \beta) = i\beta z/t + \alpha z^2 - z^4$, $2\alpha = 1/t_* - 1/t < 0$ for $0 < t < t_*$. The saddle points $z_s(\beta; t)$ are the roots of

$$0 = \frac{\partial w}{\partial z}(z, \beta) = \frac{\beta}{t}i + 2\alpha z - 4z^3. \tag{4.6}$$

Throughout the remainder of the analysis, we write $(\beta; t)$ as in $z_s(\beta; t)$ to denote that t is to be considered as a parameter. We let $z = -iu$, then u satisfies a cubic equation

with real coefficients, namely

$$u^3 + \frac{\alpha}{2}u - \frac{\beta}{4t} = 0.$$

In order to have some cancellation in the expansion of E_ν to obtain zeros, we need two equally relevant saddle points. Let $x_s(t) = t(2\alpha/3)^{3/2} = i\,(3t_*)^{-3/2}(t_* - t)^{3/2}t^{-1/2}$, then for $t < t_*$, we find that two of the saddle points come in conjugate pairs only when $|\beta| > |x_s(t)|$, where $\beta = \pm|x_s(t)|$ is the boundary of analyticity of the inviscid solution up to $t = t_*$ (see § 6). From Cardan's formula for the roots of a cubic polynomial (see (B.3)), we find

$$\text{(4.7)} \qquad \begin{cases} u_0 = \omega\mathcal{A} + \omega^2\mathcal{B} = -\frac{1}{2}(\mathcal{A}+\mathcal{B}) + i\frac{\sqrt{3}}{2}(\mathcal{A}-\mathcal{B}) \\ u_1 = \overline{u_0} = \omega^2\mathcal{A} + \omega\mathcal{B} = -\frac{1}{2}(\mathcal{A}+\mathcal{B}) - i\frac{\sqrt{3}}{2}(\mathcal{A}-\mathcal{B}) \\ u_2 = \mathcal{A} + \mathcal{B} \end{cases}$$

where $\omega = e^{2\pi i/3}$. Since $x_s^2 = -|x_s^2| < 0$ for $t < t_*$, we find

$$\text{(4.8)} \qquad \begin{aligned} &\text{for } \beta > |x_s(t)|, \quad \begin{cases} \mathcal{A}(\beta;t) = (8t)^{-1/3}\ \sqrt[3]{\beta + \sqrt{\beta^2 + x_s^2}} > 0 \\ \mathcal{B}(\beta;t) = (8t)^{-1/3}\ \sqrt[3]{\beta - \sqrt{\beta^2 + x_s^2}} > 0 \end{cases} \\ &\text{for } \beta < -|x_s(t)|, \quad \begin{cases} \mathcal{A}(\beta;t) = -(8t)^{-1/3}\ \sqrt[3]{-\beta + \sqrt{\beta^2 + x_s^2}} < 0 \\ \mathcal{B}(\beta;t) = -(8t)^{-1/3}\ \sqrt[3]{-\beta - \sqrt{\beta^2 + x_s^2}} < 0 \end{cases} \end{aligned}$$

so that

$$\text{(4.9)} \qquad z_s(-\beta;t) = -z_s(\beta;t).$$

Here we are taking the real positive branches of the square roots and cube roots in $\mathcal{A}$ and $\mathcal{B}$. We have also used the relation

$$\text{(4.10)} \qquad |x_s(t)| = t\left(\frac{2|\alpha|}{3}\right)^{3/2} = t\left(-\frac{2\alpha}{3}\right)^{3/2} > 0,$$

where we are taking the positive branch of $z^{3/2}$ for $z > 0$. Moreover when choosing the branches of the rational functions $\mathcal{A}$ and $\mathcal{B}$, one must make sure that they satisfy the relation $\mathcal{A}\cdot\mathcal{B} = -\alpha/6 > 0$ (see Appendix B). In terms of the original variable $z = -iu$, after separation of the real and imaginary parts, we have

$$\text{(4.11)} \qquad \begin{cases} z_0 = \frac{\sqrt{3}}{2}(\mathcal{A}-\mathcal{B}) + \frac{i}{2}(\mathcal{A}+\mathcal{B}) \\ z_1 = -\overline{z_0} = \frac{\sqrt{3}}{2}(\mathcal{B}-\mathcal{A}) + \frac{i}{2}(\mathcal{A}+\mathcal{B}) \\ z_2 = -i(\mathcal{A}+\mathcal{B}) \end{cases}$$

Since we are only looking at values of $|\beta| > |x_s|$, the steepest paths and level curves look almost like the case $t = t_*$ described in Fig. 4.1, except that the saddle points have moved closer together, yet preserving the symmetry of Fig. 4.1. The path deformation is justified in the same way (see [25] for more details). The saddle-points come in symmetric pairs that satisfy $z_0 = -\overline{z_1}$ for all $t > 0$. We have

$$\text{(4.12a)} \qquad 0 = \frac{\partial w}{\partial z}(z_s(\beta;t),\beta) = \frac{\beta}{t}i + 2\alpha z_s - 4z_s^3$$

$$\text{(4.12b)} \qquad 0 = \frac{1}{4}z_s\frac{\partial w}{\partial z}(z_s(\beta;t),\beta) = \frac{i\beta}{4t}z_s + \frac{\alpha}{2}z_s^2 - z_s^4$$

$$\text{(4.12c)} \qquad w(z_s(\beta;t),\beta) = \frac{i\beta}{t}z_s + \alpha z_s^2 - z_s^4$$

(4.12a) gives (4.12b), which combined with (4.12c) gives

$$w(z_s(\beta;t),\beta) = \frac{3i\beta}{4t} z_s + \frac{\alpha}{2} z_s^2. \tag{4.13}$$

Since for $s = 0, 1$

$$z_s(\beta;t) = (-1)^s \frac{\sqrt{3}}{2}(\mathcal{A} - \mathcal{B}) + \frac{i}{2}(\mathcal{A} + \mathcal{B}), \tag{4.14a}$$

$$w_{zz}(z_s,\beta) = 2\alpha - 12z_s^2, \quad w(z_0,\beta) = \overline{w(z_1,\beta)}, \tag{4.14b}$$

so that

$$\Re\, w(z_s(\beta;t),\beta) = \frac{\alpha}{4}(\mathcal{A}^2 + \mathcal{B}^2) - \frac{3\beta}{8t}(\mathcal{A} + \mathcal{B}) - \frac{\alpha^2}{6}, \tag{4.15a}$$

$$\Im\, w(z_s(\beta;t),\beta) = (-1)^s \frac{\sqrt{3}}{8} \cdot (\mathcal{A} - \mathcal{B}) \cdot (3\beta/t + 2\alpha(\mathcal{A} + \mathcal{B})), \tag{4.15b}$$

$$\theta(z_s(\beta;t),t) = \arg(-w_{zz}(z_s,\beta)) = (-1)^s \arg(6z_0^2 - \alpha). \tag{4.15c}$$

Using a standard steepest descents analysis (see [25, 33] for example), we find that

$$E_\nu(i\beta,t) = \sum_{s=0,1} \sqrt{\frac{-4\pi\nu}{w_{zz}(z_s,\beta)}}\, e^{w(z_s,\beta)/2\nu}\,(1 + \mathcal{O}(\nu)) \quad \text{as } \nu \to 0^+.$$

We can further simplify the expansion using the actual value of $\sqrt{6z_s^2 - \alpha}$. Indeed, since $z_s(\beta;t) = (-1)^s \frac{\sqrt{3}}{2}(\mathcal{A} - \mathcal{B}) + \frac{i}{2}(\mathcal{A} + \mathcal{B}) = e^{i\pi/6}\mathcal{A} + e^{i5\pi/6}\mathcal{B}$, and $\mathcal{A} \cdot \mathcal{B} = -\alpha/6$,

$$6z_s^2 - \alpha = 3\sqrt{(\mathcal{A}^2 + \mathcal{B}^2 - \alpha)^2 + 3(\mathcal{A}^2 - \mathcal{B}^2)}\, e^{i\theta(z_s(\beta;t),t)}, \tag{4.16a}$$

$$\theta(z_s(\beta;t),t) = \arg(6z_s^2 - \alpha) = (-1)^s \tan^{-1}\left(\sqrt{3} \cdot \frac{\mathcal{A}^2 - \mathcal{B}^2}{\mathcal{A}^2 + \mathcal{B}^2 + \alpha/3}\right), \tag{4.16b}$$

where in (4.16b) we are taking the branch of $\tan^{-1} x$ for which $|\tan^{-1} x| < \pi/2$. Reproducing a similar analysis for $t > t_*$, we have the following result:

THEOREM 4.3. *The asymptotic expansion of $E_\nu(i\beta,t)$ as $\nu \to 0^+$ is*

$$E_\nu(i\beta,t) = \sqrt{\frac{2\pi\nu}{|6z_s^2 - \alpha|}} \exp\left\{\frac{1}{2\nu}\,\Re\, w(z_s(\beta;t),\beta)\right\} \times \left[\cos\Big(\frac{1}{2\nu}\,\Im\, w(z_0(\beta;t),\beta) - \frac{1}{2}\theta(z_0(\beta;t),t)\Big) + \mathcal{O}(\nu)\right],$$

where

$$z_s(\beta;t) = (-1)^s \frac{\sqrt{3}}{2}(\mathcal{A} - \mathcal{B}) + \frac{i}{2}(\mathcal{A} + \mathcal{B}) \qquad \text{for } s = 0, 1,$$

and $\mathcal{A}$ and $\mathcal{B}$ are given by

$$\mathcal{A}(\beta;t) = (8t)^{-1/3} \sqrt[3]{\beta + \sqrt{\beta^2 + x_s^2}}$$

$$\mathcal{B}(\beta;t) = \begin{cases} 0 < t < t_* & (8t)^{-1/3} \sqrt[3]{\beta - \sqrt{\beta^2 + x_s^2}} > 0 \qquad \beta > |x_s| \\ t > t_* & -(8t)^{-1/3} \sqrt[3]{-\beta + \sqrt{\beta^2 + x_s^2}} < 0 \qquad \beta > 0 \end{cases}$$

For $\beta < 0$, $z_s(\beta;t)$ is defined by the odd parity condition $z_s(\beta;t) = -z_s(-\beta;t)$. Letting $t \to t_*$ in Theorem 4.3, we obtain $\theta(z_s(\beta;t_*),t_*) = (-1)^s\pi/3$, and

$$\Re\, w(z_s(\beta;t_*),\beta) = -\frac{3}{2}\left(\frac{\beta}{4t_*}\right)^{4/3},$$
$$\Im\, w(z_s(\beta;t_*),\beta) = (-1)^s\frac{3\sqrt{3}}{2}\left(\frac{\beta}{4t_*}\right)^{4/3}.$$

For small ν the poles β_k are approximated by the roots of the equation

$$\frac{1}{2\nu}\,\Im\, w(z_0(\beta;t),\beta) - \frac{1}{2}\theta(z_0(\beta;t),t) = \left(k-\frac{1}{2}\right)\pi, \quad k \in \mathbb{N}^*, \tag{4.17}$$

with the convention that $\beta_{-k} \equiv -\beta_k$. Since $|\theta(z_0(\beta_k;t),t)| < \pi$, $\forall \beta_k \in \mathbb{R}$, the limiting behavior of the poles is given by $\Im\, w(z_0(\beta;t),\beta) = 0$. Recall from (4.15b) that

$$\Im w_s = \Im\, w(z_s(\beta;t),\beta) = (-1)^s\frac{\sqrt{3}}{8}\cdot(\mathcal{A}-\mathcal{B})\cdot(3\beta/t + 2\alpha(\mathcal{A}+\mathcal{B})),$$

so that

$$\Im w_s = 0 \Leftrightarrow \begin{cases} \text{either } \mathcal{A} = \mathcal{B}, \text{or} \\ 3\beta/t + 2\alpha(\mathcal{A}+\mathcal{B}) = 0, \end{cases} \tag{4.18}$$

For $0 < t \leqslant t_*$, $\alpha \leqslant 0$: If $\beta \geqslant |x_s|$ then $\mathcal{A} > 0, \mathcal{B} > 0$, and if $\beta \leqslant |x_s|$ then $\mathcal{A} < 0, \mathcal{B} < 0$. We re-write the second equation as $(\mathcal{A}+\mathcal{B})^3 = -(3\beta/2\alpha t)^3$, which, after expanding the l.h.s. and using the fact that $\mathcal{A}\cdot\mathcal{B} = -\alpha/6$, reduces to $\beta = \pm|x_s(t)|$. The same conclusion is reached from the first equation $\mathcal{A} = \mathcal{B}$. Thus for $0 < t \leqslant t_*$, $\Im w_s = 0$ only if $\beta = \pm|x_s|$. Let $\hat{\beta} \ll \beta$, then re-substituting $\beta = |x_s(t)| + \hat{\beta}$ into the expansion for $E_\nu(i\beta,t)$ in Theorem 4.3, and reproducing an analysis which is similar to the one described in [25] (i.e. inverting the asymptotic series expansion), we find that the error term is $\mathcal{O}\left((k\nu)^{3/4}\right)$. Thus we can write that $\beta_{\pm k}(t,\nu) = \pm|x_s| + \mathcal{O}\left((k\nu)^{3/4}\right)$ as $\nu \to 0^+$ for fixed k. Similarly for $t \geqslant t_*$, $\alpha \geqslant 0$, $\beta > 0 \Rightarrow \mathcal{A}-\mathcal{B} > 0$, and $\beta < 0 \Rightarrow \mathcal{A}-\mathcal{B} < 0$, hence $\Im w_s = 0 \Leftrightarrow \beta = 0$ as a result of setting $3\beta/t + 2\alpha(\mathcal{A}+\mathcal{B}) = 0$. Since $\Im x_s(t) = 0$ for $t \geqslant t_*$, we have proved the following (see Fig. 5.12):

COROLLARY 4.4. *For all $t > 0$, the small viscosity ($\nu \to 0^+$) behavior of the poles $x = \pm a_k(t,\nu) = \pm i\beta_k(t,\nu)$ is*

$$\beta_k(t,\nu) = \Im x_s(t) + \mathcal{O}\left((k\nu)^{3/4}\right).$$

Of particular interest is the modulus of the first ordered pole $\beta_1(t,\nu)$ which governs the time evolution of the width of the analyticity strip of the viscous solution.

5. Numerics.

5.1. Finite difference approximation, asymptotic approximation and pole expansion. We present a numerical scheme which enables us to solve (1.1) for moderately small values of ν. The procedure is sometimes referred to as the method of lines and consists in using a centered difference operator in space while time-marching with a Runge-Kutta scheme. The method is implemented on the interval $I = [0, 1/2]$, with boundary conditions

$$u_\nu(0,t) = u_\nu(1/2,t) = 0. \tag{5.1}$$

The boundary condition $u_\nu(1/2,t)=0$ is chosen so as to be consistent with the zero value of the inviscid solution $u(1/2,t)$. Thus we can expect the difference approximation to be consistent with the initial (boundary) value problem for small ν. Two different initial conditions are also used:

$$u(x,0)=u_\nu(x,0)=4x^3-\frac{x}{t_*}, \tag{5.2a}$$

$$u_\nu(x,t_*)=\frac{x}{t_*}-\sum_{n=1}^{\infty}\frac{4\nu x}{x^2+\beta_n^2(t_*,\nu)}. \tag{5.2b}$$

Throughout the numerics we use the parameter value $t_*=1$. If the second condition is used, then the pole positions at $t=t_*$ are specified by the asymptotic estimate presented in Theorem 4.2. This estimate is used for all values of μ_n for $10\leqslant n\leqslant N$:

$$\begin{cases}\beta_n(t_*,\nu)=4t_*(2\nu\mu_n)^{3/4},\\ \mu_n=G(\mu_n^{(0)}),\quad \mu_n^{(0)}=\frac{2\pi}{3\sqrt{3}}(n-1/3),\quad n\geqslant 10,\\ G(\mu)=\mu+\frac{7}{432\mu}\left(1-\frac{1}{6\mu}\left(1+\frac{7}{72\mu}\left(1-\frac{5}{12\mu}\left(1+\frac{53143}{18900\mu}\right)\right)\right)\right),\end{cases} \tag{5.3}$$

For $1\leqslant n\leqslant 9$, we use the numerical values found in [25, Table 3], under the column "Numerical roots":

$$\begin{aligned}&\mu_1=0.8221037147 \quad \mu_2=2.0226889660 \quad \mu_3=3.2292915284\\ &\mu_4=4.4372464748 \quad \mu_5=5.6457167459 \quad \mu_6=6.8544374340\\ &\mu_7=8.0632985369 \quad \mu_8=9.2722462225 \quad \mu_9=10.4812510479.\end{aligned} \tag{5.4}$$

Let

$$\begin{aligned}&u_j=u_\nu(j*\Delta x,t),\quad Ev_j=v_{j+1},\quad E^pv_j=v_{j+p},\\ &D_+=(E-E^0)/\Delta x,\quad D_-=(E^0-E^{-1})/\Delta x,\quad D_0=(D_++D_-)/2.\end{aligned}$$

One then solves the system of N_x-1 equations using a Runge-Kutta 4-5 scheme (which we refer to as RK45):

$$\begin{cases} du_j/dt &= -D_0(u_j^2/2)+\nu D_+D_-u_j, \qquad j=1,\cdots,N_x-1,\\ u_{j=0} &= u_\nu(0,t)=0, \qquad u_{j=N_x}=u_\nu(1/2,t)=0\end{cases} \tag{5.5}$$

where N_x is the number of gridpoints (and grid-functions), and $N_x*\Delta x=1/2$. Typically the mesh size we use is $\Delta x=.25\times 10^{-2}$ and $N_x=200$ gridpoints. The time stepping restrictions depend on the size of ν and on how far in time one wants to go. For example if the final time is $t=t_*=1$, whether $\nu=10^{-2}$ or $\nu=10^{-3}$, it suffices to use $\Delta t=.25\times 10^{-2}$, $N_t=400$ RK45 steps. However, for $\nu=10^{-2}$, if one wants to go as far as $t=2$, for reasons of stability one needs to use a smaller time step such as $\Delta t=10^{-3}$, $N_t=2{,}000$. The domain of integration is $(x,t)\in[0,1/2]\times[0,T]$, where $T=1$ or $T=2$. Then due to the odd parity of the solution we reflect symmetrically for $x\in[-1/2,0]$ according to the rule $u_\nu(-x,t)=-u_\nu(x,t)$. This finite difference scheme is used in order to compare the predictions obtained from the pole expansion and the pole dynamics in § 5.2.

5.2. Numerical pole dynamics. We investigate the motion of the simple poles of $u_\nu(x,t)$ by solving the truncated Calogero dynamical system, and by starting with initial data for the poles at $t = t_*$. The poles of $u_\nu(x,t)$ are located at $\pm a_n(t,\nu) = \pm i\sqrt{\nu\gamma_n(t,\nu)}$, where the variables $\gamma_n(t,\nu) > 0$ satisfy the system (cf. Property 2.2)

$$\forall n \in \mathbb{N}, \quad \begin{cases} \dfrac{\dot\gamma_n}{2} = \dfrac{\gamma_n}{t} + 1 - 4\,\gamma_n \sum_{l\neq n} \dfrac{1}{\gamma_l - \gamma_n}, \\ \gamma_n(t_*,\nu) = (4t_*)^2\,(2\mu_n)^{3/2}\sqrt{\nu} \end{cases} \tag{5.6}$$

In order to solve this system we use the asymptotic estimate for μ_n presented in (5.3) and the numerical values of (5.4). We are mainly interested in describing the motion of the first pole $a_1(t,\nu) = i\beta_1(t,\nu) \in i\mathbb{R}$; this amounts to describe the time evolution of the width of the strip of analyticity of the solution $u_\nu(t,x)$. The imaginary part of the poles $\beta_n(t,\nu)$ is recovered using the relation $\beta_n(t,\nu) = \sqrt{\nu\gamma_n(t,\nu)}$. We plot the evolution of $\beta_n(t,\nu), n = 1,\cdots,4$ for different values of ν. We use N poles in the computations, i.e. β_1 through β_N where $N \times 10^{-4}$ varies from $.1, .5, 1, 2.5, 5$. That is, we consider the truncated system

$$\forall n = 1,\cdots,N, \quad \begin{cases} \dfrac{\dot\gamma_n}{2} = \dfrac{\gamma_n}{t} + 1 - 4\gamma_n \sum_{\substack{l=1 \\ l\neq n}}^{N} \dfrac{1}{\gamma_l - \gamma_n} \\ \gamma_n(t_*,\nu) = (4t_*)^2(2\mu_n)^{3/2}\sqrt{\nu} \end{cases}$$

In order to accelerate the computation of the slowly converging pole expansions which require $\mathcal{O}(N^2)$ operations

$$\sum_{\substack{l=1 \\ l\neq n}}^{N} \frac{1}{\gamma_l - \gamma_n}, \qquad \forall n = 1,\cdots,N, \tag{5.7}$$

we use a Multipole algorithm developped and implemented by Greengard and Rokhlin [19] which reduces the computational complexity to $\mathcal{O}(N\log N)$. A fourth/fifth order Runge-Kutta-Fehlberg scheme with automatic step-size control is used (the same one that is used for the finite difference scheme/method of lines computations of the previous section). Since the initial data is specified at $t = t_* = 1$, we can solve the system forward and backwards in time starting from $t = 1$. The typical bound on the relative error in the computation is $10^{-8} < |\frac{x_4 - x_5}{x_5}| < 10^{-4}$ where x_4 and x_5 are respectively the fourth and fifth order estimates of $\gamma_1(t,\nu)$. Once this error criterion is met, we recover the pole location via the relation $a_n(t,\nu) = i\sqrt{\nu\gamma_n(t,\nu)}$. The justification of the numerics is the most difficult aspect of this simulation because one must justify the convergence of the method both as the number of poles increases and as the time step is refined. The time-step control is automatically determined by the local relative tolerance (L.R.T. $= |\frac{x_4 - x_5}{x_5}|$) test on the 4-th and 5-th order approximations of the first ordered pole (the one closest to the origin). Thus one cannot fix the time stepping, rather one can have a subtle control on it by reducing this tolerance. Typically, we fix the number of poles to $N = 50,000$ and vary the tolerance on the successive intervals $10^{-10} < L.R.T. < 10^{-6}$, $10^{-8} < L.R.T. < 10^{-4}$, $10^{-6} < L.R.T. < 10^{-2}$. Then we fix the tolerance at the highest reasonable level $10^{-8} < L.R.T. < 10^{-4}$, and vary the number of poles where $N \times 10^{-4}$ is either $.1, .5, 1, 2.5$ or 5. We see that the time step barely affects the convergence of the method. Thus the main difficulty in this procedure arises from the slow convergence of the pole interaction (5.7) that is present in the Calogero dynamical system.

5.2.1. 2-pair pole-dynamics test. In order to verify the accuracy of the numerical pole dynamics, we implement the numerical method described in the previous section for the case where there are only four poles (2 pairs). In this case, one can explicitly solve the resulting system as follows: Let $a_n = i\beta_n$, that is replace β_n by $-ia_n$ in system (2.17) so that the two pairs of poles $\{(-a_1, a_1), (-a_2, a_2)\}$ and $\{(-\kappa_1, \kappa_1), (-\kappa_2, \kappa_2)\}$ satisfy, under the transformation $\kappa_n = a_n^2/\nu$, the equivalent systems

$$\begin{cases} \dot{a}_1 = a_1/t - \nu/a_1 - 4\nu a_1/(a_1^2 - a_2^2) \\ \dot{a}_2 = a_2/t - \nu/a_2 + 4\nu a_2/(a_1^2 - a_2^2) \end{cases} \iff \begin{cases} \dot{\kappa}_1/2 = \kappa_1/t - 1 - 4\kappa_1/(\kappa_1 - \kappa_2) \\ \dot{\kappa}_2/2 = \kappa_2/t - 1 + 4\kappa_2/(\kappa_1 - \kappa_2) \end{cases}$$

Introduce a set of new variables $\{\Theta_1,\Theta_2\}$ defined by

$$\begin{cases} \Theta_1 = \kappa_1 + \kappa_2 \\ \Theta_2 = \kappa_1 - \kappa_2 \end{cases} \iff \begin{cases} \kappa_1 = (\Theta_1 + \Theta_2)/2 \\ \kappa_1 = (\Theta_1 - \Theta_2)/2 \end{cases}$$

Then it is easy to show that $\{\Theta_1,\Theta_2\}$ satisfy the coupled system of nonlinear ODEs

$$\begin{cases} \dot{\Theta}_1 - 2\Theta_1/t = -12 \\ \dot{\Theta}_2 - 2\Theta_2/t = -8\Theta_1/\Theta_2 \end{cases} \tag{5.8}$$

We further introduce a new variable denoted by $\phi_2 = \Theta_2^2$ which in turn satisfies the linear ODE

$$\dot{\phi}_2 - 4\phi_2/t = -16\Theta_1. \tag{5.9}$$

We use as initial data the position of the poles $a_1(t_*, \nu) = i\beta_1(t_*, \nu)$ and $a_2(t_*, \nu) = i\beta_1(t_*, \nu)$, where $\beta_1(t_*, \nu)$ and $\beta_2(t_*, \nu)$ are given in (5.3) and (5.4). Thus we have

$$\begin{cases} \Theta_1^* = \Theta_1(t_*, \nu) = \kappa_1(t_*, \nu) + \kappa_2(t_*, \nu) = a_1^2(t_*, \nu)/\nu + a_2^2(t_*, \nu)/\nu \\ \phi_2^* = \phi_2(t_*, \nu) = \Theta_2^2(t_*, \nu) = (a_1^2(t_*, \nu)/\nu - a_2^2(t_*, \nu)/\nu)^2 \end{cases} \tag{5.10}$$

Solving the initial value problem consisiting of the first equation in system (5.8), equations (5.9) and (5.10), we find that

$$\begin{cases} \Theta_1(t, \nu) = (t/t_*)^2\Theta_1^* - 12t(t - t_*)/t_* \\ \phi_2(t, \nu) = (t/t_*)^4 (\phi_2^* - 16t_*(t - t_*)(t\Theta_1^* - 6tt_* + 6t_*^2)/t^2) \end{cases} \tag{5.11}$$

Taking $t_* = 1$, $\nu = .001$, we use (5.11), a straightforward numerical integration scheme using Runge-Kutta 4-5, and Runge-Kutta 4-5 together with the Multipole algoritm in which we set to zero all coefficients pertaining to $a_n, n \geqslant 3$. We find common values for all three methods at $t = 1.25$:

$$\begin{cases} a_1(t = 1.25, \nu = .001) = 0.0408023705 * i \\ a_2(t = 1.25, \nu = .001) = 0.1009178717 * i \end{cases} \tag{5.12}$$

Computing the differences between the exact values of a_1 and a_2 and the predictions obtained from the Runge-Kutta schemes (with and without the Multipole algorithm), we find that these predictions are of the order of $\mathcal{O}(10^{-10})$ which is consistent with the expected 4-th order accuracy of such numerical schemes.

5.3. Figures, descriptions and comparisons. All the numerics that are described in this section are done in DOUBLE PRECISION Fortran on a Sun Sparcstation 1,000 (Scorpion).

In Fig. 5.1, we illustrate the "slow" convergence of the pole expansion as the viscosity decreases. In particular, for $\nu = 10^{-4}$ and 10^{-5}, we can compare the inviscid solution given by (see (6.4) and (6.8))

$$u(x, t_*) = \frac{x}{t_*} - (\frac{x}{4t_*})^{1/3}, \tag{5.13}$$

to the pole expansion, and expect good agreement between the two. For ν very small, we see that even for a very large number of poles ($N = 10^6$) the tails of the pole expansion still do not match the true solution which is expected to be very close to the inviscid one. In each of these figures, there are five curves, four of which are computed from the pole expansion for increasing number of poles $N = 10^3, 10^4, 10^5, 10^6$. The fifth (dotted curve) is the inviscid solution at t_*.

In Figs. 5.2 and 5.3 we present comparisons between the finite difference scheme and the pole expansion ($N = 10^6$ poles) at the fixed time t_*. For the finite difference scheme, we use $N_x = 200$ points, $\Delta x = .25 * 10^{-2}$, $N_t = 400$ RK45 steps with $\Delta t = .25 * 10^{-2}$.

In Figs. 5.4 and 5.5 we present comparisons between the finite difference scheme and the saddle point approximation at the successive times $t = 1, 1.5, 2$. The mesh size is the same as the one for Figs. 5.2 and 5.3. One can observe that the saddle point approximation overshoots the true value of the solution which is best captured by the difference scheme. This overshoot is due to the degeneracy of the saddle point formula at the caustic and innacuracies around it. The correct behavior in a neighborhood of this caustic can only be correctly described by the uniform asymptotic expansion of § 3.3.

In Figs. 5.6 and 5.7, we compare the difference method and the pole dynamics for $\nu = 10^{-3}$ with $N = 50,000$ poles at the times $t = .5, 1, 1.5, 2$. The pole dynamics is run forward and backwards in time starting from $t = t_* = 1$ until $t = .5$ and $t = 2$. The solution is then re-constructed from the pole expansion and the pole locations at these specific times, and is compared to the finite difference approximations with mesh size $N_x = 200$ points, $\Delta x = .25 * 10^{-2}$, $N_t = 2,000$ RK45 time steps with $\Delta t = 10^{-3}$. The agreement between the finite difference and the pole dynamics close to the shock region is very good as opposed to the tails. Since the pole dynamics simulation involved only $50,000$ poles in Fig. 5.6, the mismatch in the tail is characteristic of the slow convergence of the pole expansion in the tails that is displayed in Fig. 5.1 for $\nu = 10^{-3}$. There is also a small source of error in the difference scheme where the boundary condition at $x = 1/2$ is set to the inviscid value ($u(1/2, t) = 0$). This error in the difference approximation increases for larger ν. Thus the discrepancy observed in the tails of the solution in Fig. 5.16 is more likely to arise from errors in the difference scheme than the pole dynamics. Indeed, it suffices to look at the convergence of the pole expansion at $t = t_*$ in Fig. 5.1, $\nu = 10^{-2}$, to establish confidence in the pole dynamics.

However, one can notice that regardless of the size of ν (whether $\nu = 10^{-2}$ or 10^{-3}), within the shock region of width $\mathcal{O}(\nu)$, the agreement between the pole dynamics and the difference approximation is very good (see Figs. 5.3, 5.17). This shows that the dynamics of the first few poles is accurately captured by the pole dynamics. This also

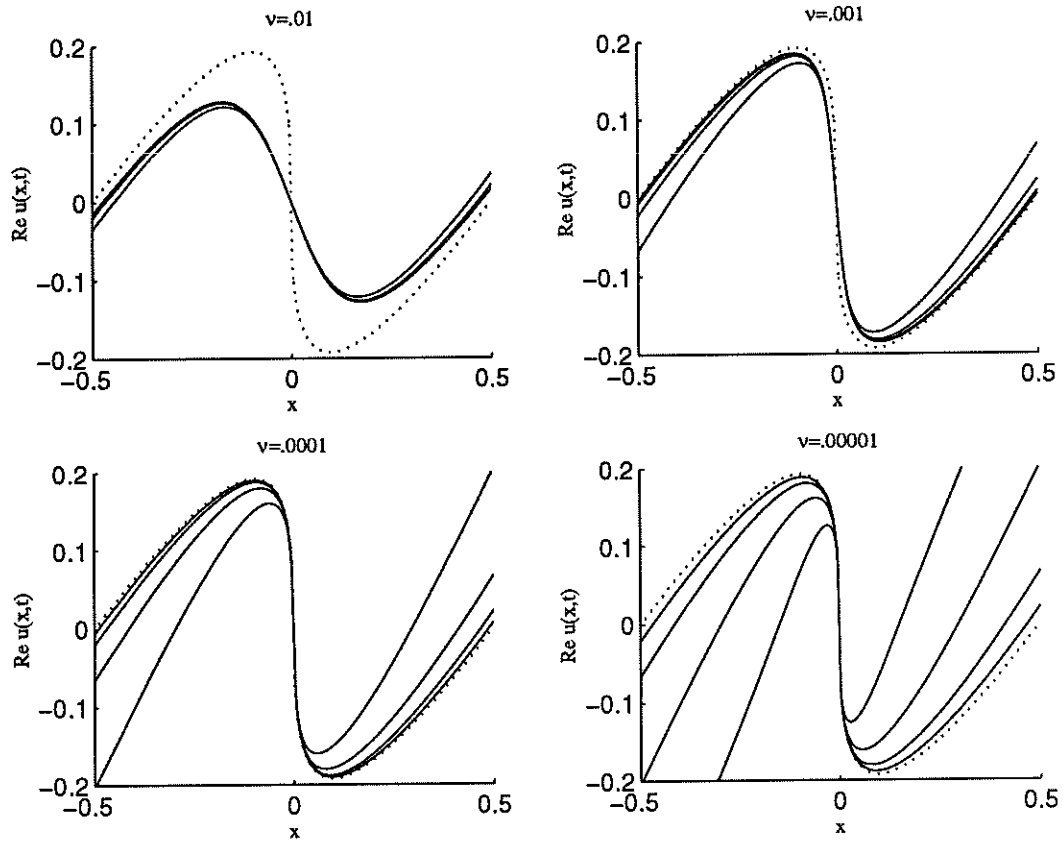

FIG. 5.1. *Convergence of the pole expansion as* $N \to +\infty$ *of the solution* $u_\nu(x,t_*) = x/t_* - \sum_{n=1}^{N} 4\nu x/(x^2+\beta_n^2(t_*,\nu))$ *with varying number of poles ranging from* $N = 10^3, 10^4, 10^5, 10^6$ *poles for* $\nu = 10^{-2}, 10^{-3}, 10^{-4}, 10^{-5}$. *The dotted curve is computed from the inviscid solution at* $t = t_* = 1$ *by* $u(x,t_*) = x/t_* - (x/4t_*)^{1/3}$. *For* $\nu = 10^{-2}$, *the inviscid solution and the pole expansion* $u_\nu(x,t_*)$ *do not agree because the viscosity is large enough that the solution has started decaying earlier (see comments on the turn around time of the poles and their relation to the decay of the solution).*

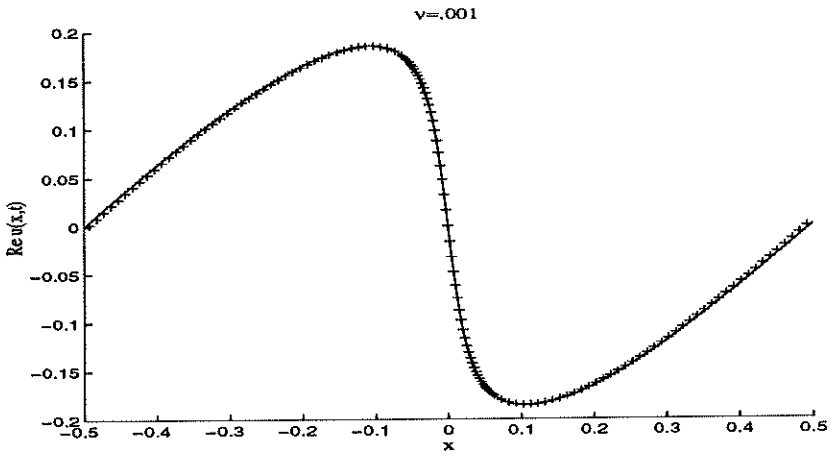

FIG. 5.2. *Comparison of the solution reconstruction at* $t = t_* = 1$ *from the pole expansion* $u_\nu(x,t_*) = x/t_* - \sum_{n=1}^{N} 4\nu x/(x^2+\beta_n^2(t_*,\nu))$ *with* $N = 10^6$ *poles, and the finite difference scheme (method of lines) for* $\nu = 10^{-3}$. *Mesh size:* $N_x = 200$ *points,* $\Delta x = .25 * 10^{-2}$, $N_t = 400$ *RK45 time steps with* $\Delta t = .25 * 10^{-2}$. *Pole expansion (+) at* $t = 1$ *overlaps finite difference approximation in solid curve.*

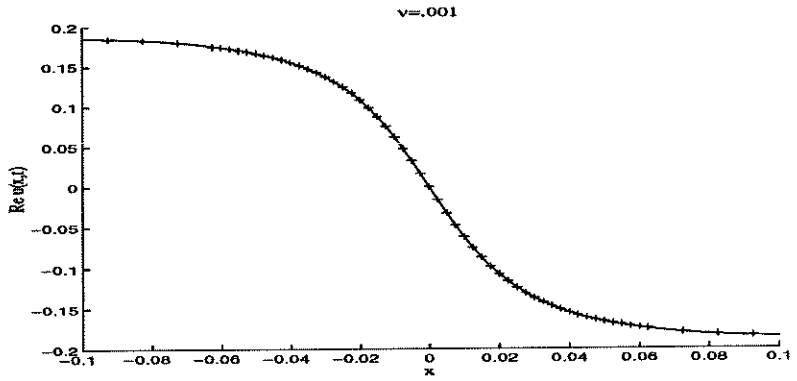

FIG. 5.3. *Closeup of Fig. 5.2 in* $[-.1,.1]$.

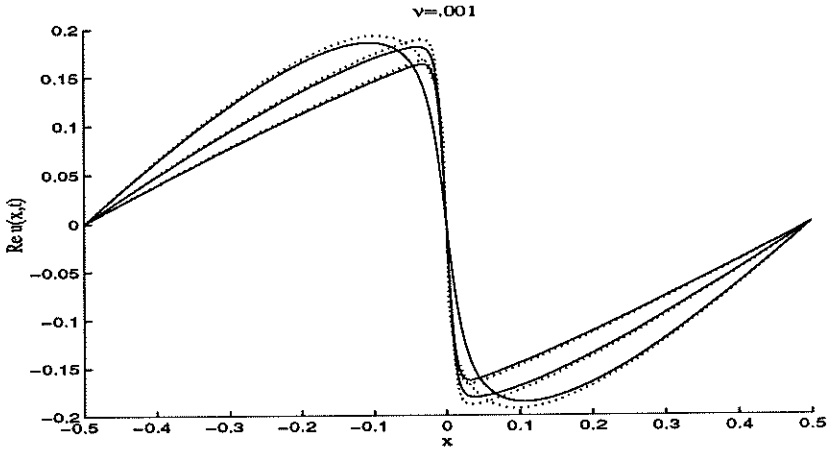

FIG. 5.4. *Comparison of finite difference scheme and saddle point method for* $\nu = 10^{-3}$ *at* $t = 1, 1.5, 2$. *Solid curves: Finite difference scheme with* $N_x = 200$ *points,* $\Delta x = .25 * 10^{-2}$, $N_t = 800$ *RK45 time steps with* $\Delta t = .25 * 10^{-2}$. *Dotted curves: Saddle point approximation overshooting the finite difference approximation.*

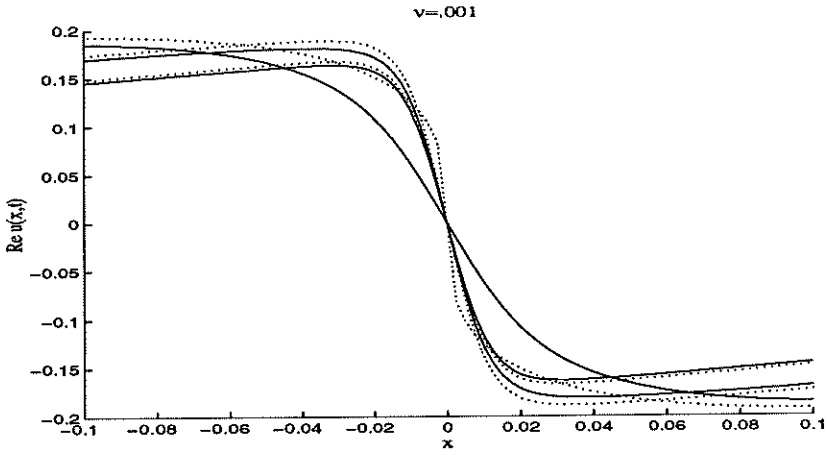

FIG. 5.5. *Closeup of Fig. 5.4 in* $[-.1,.1]$.

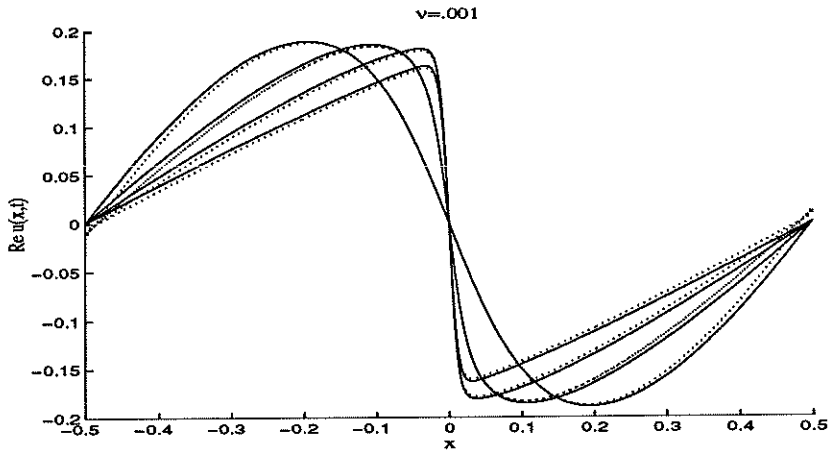

FIG. 5.6. *Comparison of the finite difference approximation (solid) and the pole dynamics (dotted) for* $\nu = 10^{-3}$ *at* $t = .5, 1, 1.5, 2$. *Finite difference mesh size:* $N_x = 200$ *points,* $\Delta x = .25 * 10^{-2}$, $N_t = 2,000$ *RK45 steps with* $\Delta t = .5{*}10^{-2}$. *Pole dynamics:* $N = 5{*}10^4$ *poles,* $10^{-8} < L.R.T. < 10^{-4}$, *typical timestep* $\Delta t = .05$, $N_t = 45$ *RK45 time steps (25 steps backwards and 20 steps forward from* $t = t_*$*).*

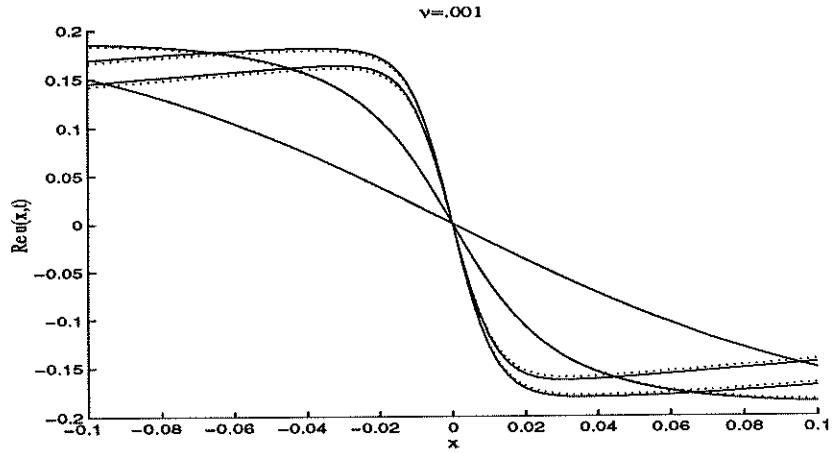

FIG. 5.7. *Closeup of Fig. 5.6 in* $[-.1, .1]$.

becomes apparent when comparing the simulations done with varying number of poles (see Figs. 5.10 and 5.11). Finally it should be noted that increasing the step-size of the time increment (in a reasonable way) in the pole dynamics barely affects the computations (see Figs. 5.8 and 5.9).

We plot the evolution of the first four (ordered) poles on the imaginary axis ($\beta_k, k = 1, \cdots, 4$), and focus on the "turn around" times t_u, and the position of the first ordered pole β_1 which determines the width of the analyticity strip. One can see that the behavior of the pole β_1 displayed in Figs. 5.8 and 5.14 is qualitatively similar to the one obtained by Sulem *et altri* in [29, III-B,Figure 3] using spectral methods for the initial data $u_0(x) = \sin(x)$ with $\nu = .05$. The most important feature in the behavior of the first ordered pole is clearly the fact that it turns around before crossing the real axis, thus preserving the uniform analyticity of the viscous solution within the strip $|\Im x| \leqslant \delta_1 < \beta_1$ where $\beta_1(t, \nu) > 0$, $\forall t > 0$. Moreover it is interesting to notice

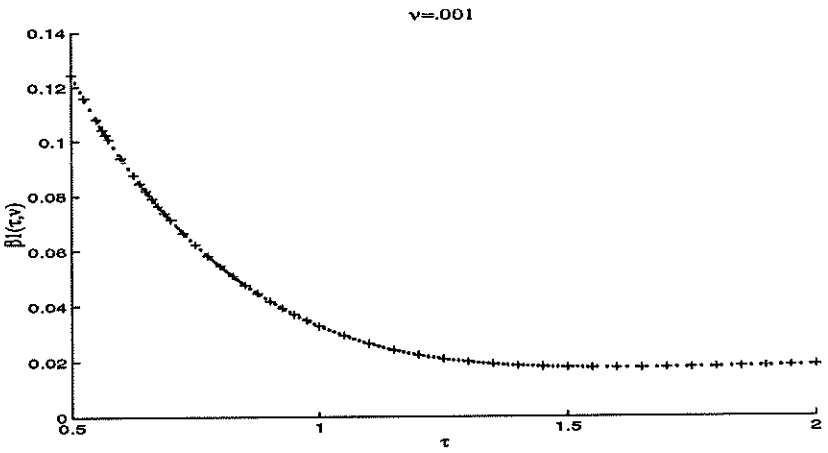

FIG. 5.8. *$\beta_1(t,\nu)$ vs. t. Time evolution in $\mathbb{R}$ of the width of the analyticity strip $\beta_1(t,\nu)$, for $\nu = 10^{-3}$ and $N = 5 \times 10^4$ poles. $t_{initial} = t_* = 1$ and $t \in [.5, 2]$. (+): $\Delta t = .05$; dots (.): $\Delta t = .01$. Both curves are indistinguishable.*

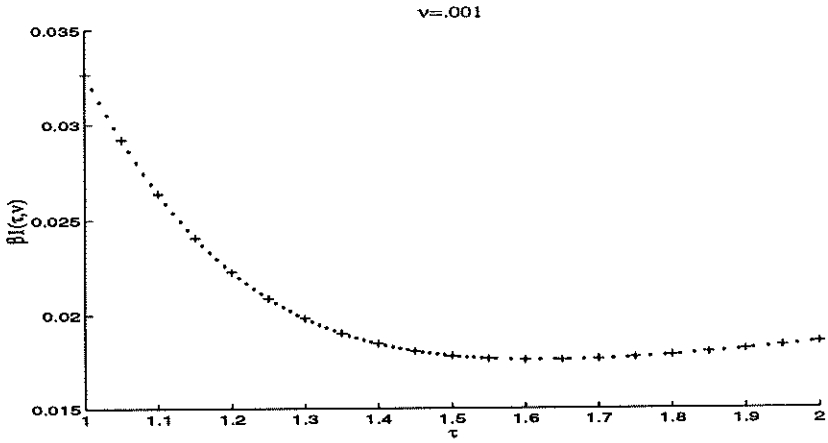

FIG. 5.9. *Closeup of Fig. 5.8 for $t \in [1, 2]$..*

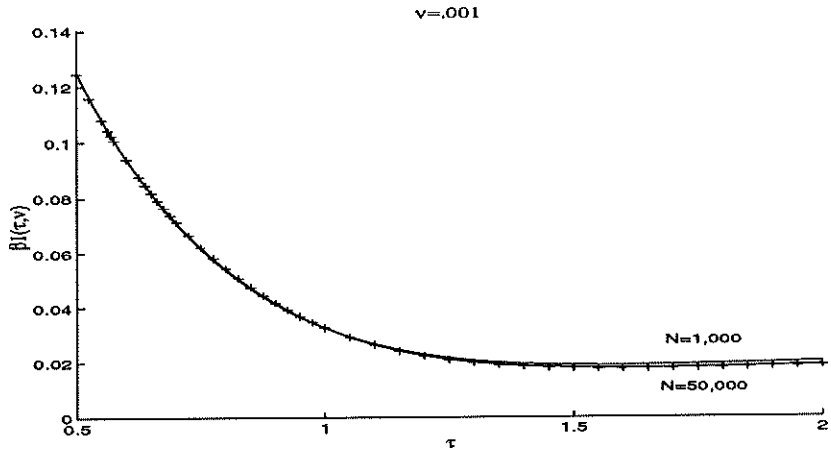

FIG. 5.10. *$\beta_1(t,\nu)$ vs. t. Comparison of pole number simulations for $\nu = 10^{-3}$ and $N = .1, .5, 1, 2.5, 5 \times 10^4$ poles. (+): $N = 5 \times 10^4$ poles; (solid): $N = .1, .5, 1, 2.5 \times 10^4$ poles. Differences appear more clearly in the closeup in Fig. 5.11.*

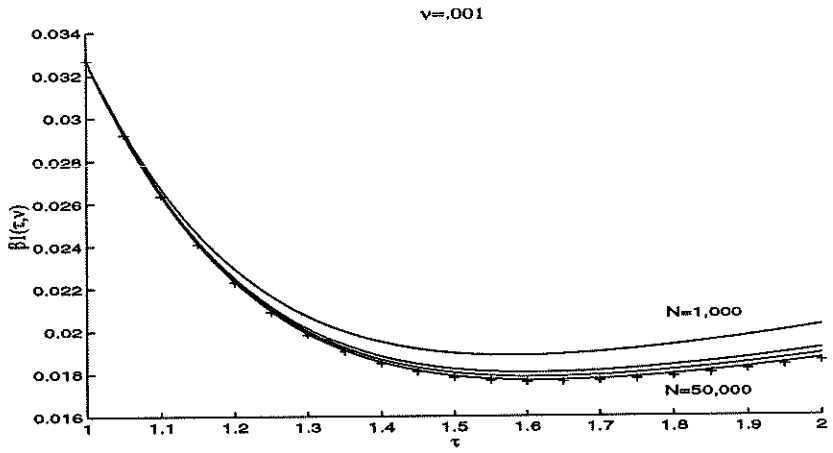

FIG. 5.11. *Closeup of Fig. 5.10 for* $t \in [1,2]$. *Turnaround time at* $t_u \approx 1.62$.

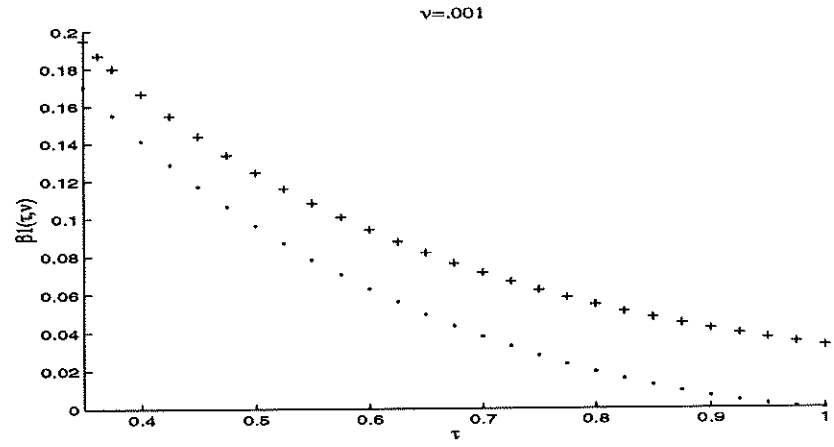

FIG. 5.12. *Comparison of the time evolutions of* $\beta_1(t, \nu = 10^{-3})$ *(+), and* $x_s(t)$ *(.) for* $t \in [.35, t_* = 1]$. *The pole dynamics is the same as Fig. 5.8 with* $N = 5 \times 10^4$ *poles. This illustrates the asymptotic relation* $\beta_1(t,\nu) = \Im x_s(t) + \mathcal{O}(\nu^{3/4})$ *as* $\nu \to 0^+$ *when* $t \leqslant t_*$ *(see Cor. 4.4).*

that the turn around times t_u for the poles β_k decrease as the index k increases. In this respect, the last pole to turn around is the first ordered pole β_1, i.e. the one closest to the real axis. For $\nu = 10^{-3}$, the turnaround times for $\beta_j, j = 1, \cdots, 4$ are at $t \approx 1.62, 1.51, 1.39, 1.27$ respectively. For $\nu = 10^{-2}$, the turnaround times for $\beta_j, j = 1, \cdots, 4$ are at $t \approx 1.05, .55, .425, .325$ respectively. Thus, comparing Figs. 5.13 and 5.15, one can see that the turn around times t_u increase with decreasing ν. That is, one can relate the time of initial decay of the solution to the turn around times t_u by comparing the evolution of the poles (Figs. 5.13, 5.15) to the correponding evolution of the solution (Figs. 5.6, 5.16).

6. Inviscid solution $(\nu = 0)$. The inviscid Burger's equation $(\nu = 0)$

$$\begin{cases} u_t + u\, u_x = 0 \\ u(x,0) = u_0(x) = 4x^3 - x/t_* \end{cases} \tag{6.1}$$

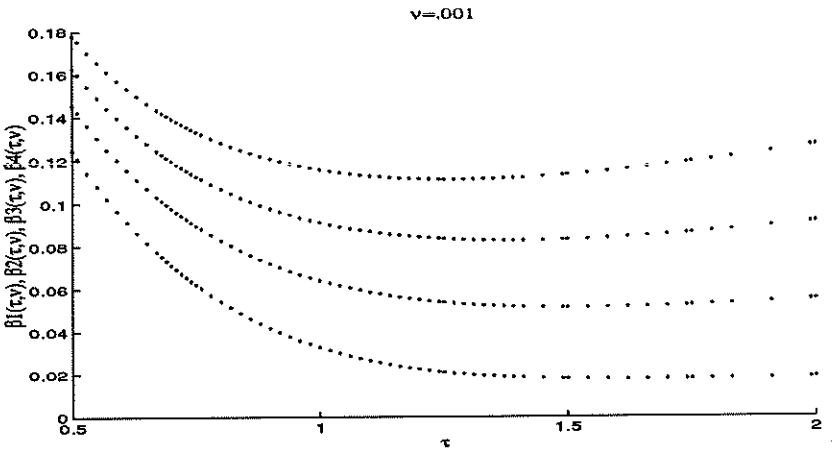

FIG. 5.13. *$\beta_j(t,\nu)$ vs. t for $j = 1, \cdots, 4$. $\nu = 10^{-3}$ and $N = 5 \times 10^4$ poles. Same parameters as in Fig. 5.8. Turn around times at $t_u \approx 1.62$, $t_u \approx 1.51$, $t_u \approx 1.39$, $t_u \approx 1.27$ for $\beta_j(t,\nu), j = 1, \cdots, 4$.*

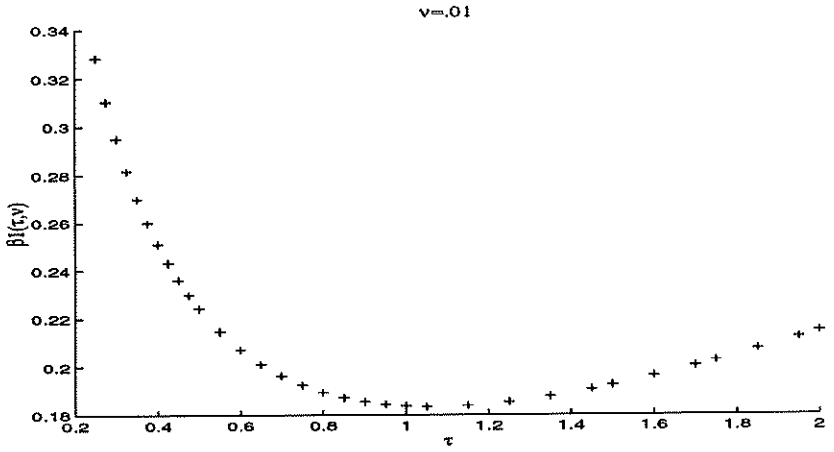

FIG. 5.14. *$\beta_1(t,\nu)$ vs. t. Time evolution in $\mathbb{R}$ of the width of the analyticity strip $\beta_1(t,\nu)$, for $\nu = 10^{-2}$ and $N = 5 \times 10^4$ poles. $t_{initial} = t_* = 1$ and $t \in [.25, 2]$. $N_{steps} = 32$ (20 steps backwards and 12 steps forward from $t = t_*$). Local relative tolerance: $10^{-10} < L.R.T < 10^{-6}$.*

states that the velocity of a fluid particle is conserved along certain trajectories, namely the characteristic lines

$$\dot{x} = \frac{dx}{dt}(t) = u(x(t),t) = u_0(x_0(x,t)) \tag{6.2}$$

in the (x,t) plane. The implicit solution obtained by the method of characteristics reflects the conservation of the velocity along these special curves:

$$\begin{cases} u = u(x,t) = u_0(x_0(x,t)) \\ x = x_0 + t\, u_0(x_0(x,t)) \end{cases} \tag{6.3}$$

A fluid particle originally at a (Lagrangian) position x_0 in space will be at a new (Eulerian) position x after a certain time t with the same velocity along this line. We can express (6.3) as

$$\begin{cases} u(x,t) = x/t - U(x,t)/t \\ U(x,t) = x_0(x,t) \end{cases} \tag{6.4}$$

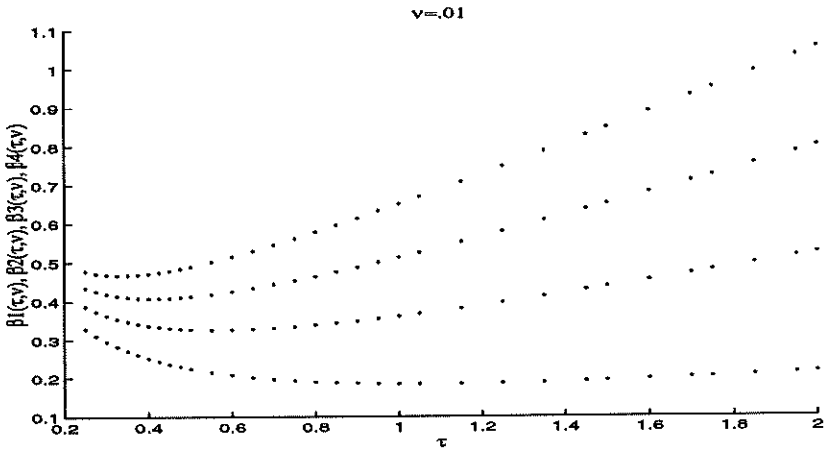

FIG. 5.15. *$\beta_j(t,\nu)$ vs. t for $t \in [.25, 2]$ and $j = 1, \cdots, 4$. $\nu = 10^{-2}$ and $N = 5 \times 10^4$ poles. Same parameters as in Fig. 5.14. Turn around times at $t_u \approx 1.05$, $t_u \approx .55$, $t_u \approx .425$, $t_u \approx .325$ for $\beta_j(t,\nu), j = 1, \cdots, 4$.*

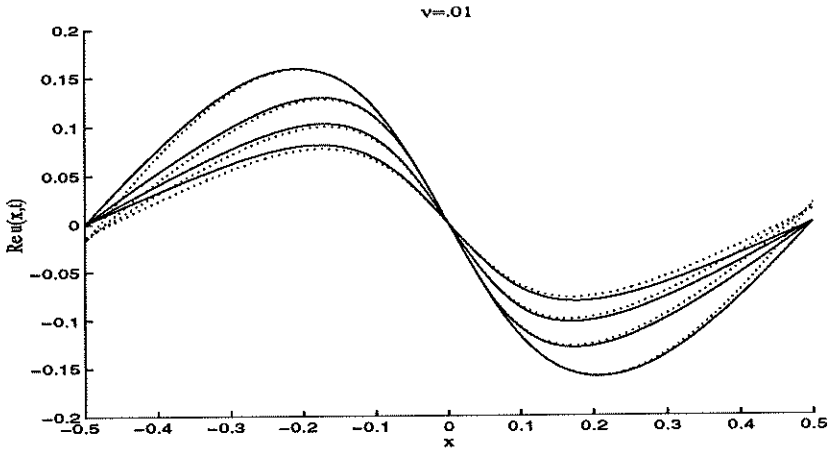

FIG. 5.16. *Comparison of the finite difference approximation (solid) and the pole dynamics (dotted) for $\nu = 10^{-2}$ at $t = .5, 1, 1.5, 2$. Finite difference mesh size: $N_x = 100$ points, $\Delta x = .5 * 10^{-2}$, $N_t = 2,000$ RK45 time steps with $\Delta t = 10^{-3}$. Pole dynamics: same as Fig. 5.14*

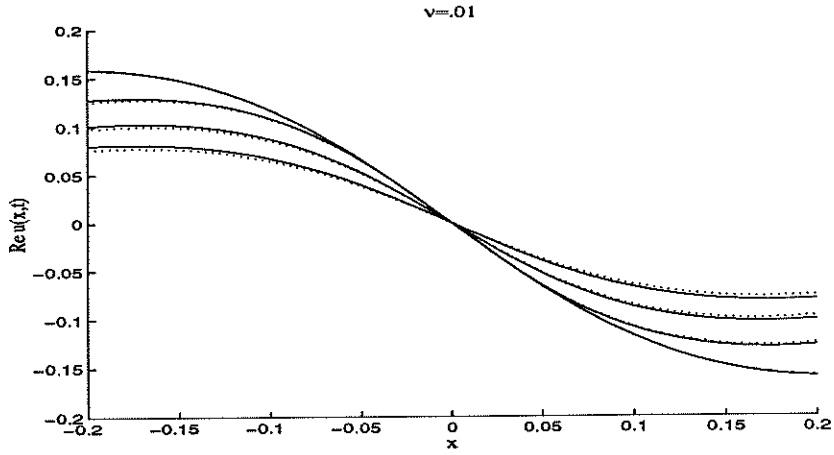

FIG. 5.17. *Closeup of Fig. 5.6 in* $[-.2, .2]$.

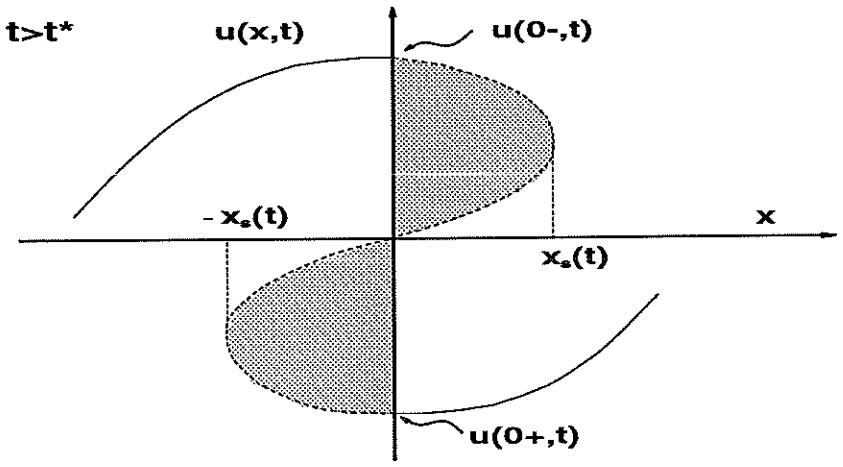

FIG. 6.1. *Shock, multi-valuedness, branch points and Maxwell's equal area rule for $t > t_*$.*

Substituting $u_0(x)$ in (6.3), we find that U satisfies the cubic equation

$$U^3 - \frac{\alpha}{2}U - \frac{x}{4t} = 0, \qquad \alpha = \frac{t - t_*}{2tt_*}. \tag{6.5}$$

This defines a three-sheeted Riemann surface for the solution with a third order branch point at infinity and two opposite second order branch points at $\pm x_s(t)$ defined by

$$x_s(t) = t(2\alpha/3)^{3/2} = \begin{cases} i(3t_*)^{-3/2}(t_* - t)^{3/2}t^{-1/2} \in i\mathbb{R} & 0 < t \leqslant t_* \\ (3t_*)^{-3/2}(t - t_*)^{3/2}t^{-1/2} \in \mathbb{R} & t \geqslant t_* \end{cases} \tag{6.6}$$

The envelope of the characteristic lines is given by the branch point:

$$\begin{aligned} 0 = \frac{\partial x}{\partial x_0} = \frac{\partial x}{\partial U} &\Rightarrow x_0 = x_0^{\pm}(t) = \pm\sqrt{\frac{t - t_*}{12tt_*}} = \pm\sqrt{\frac{\alpha}{6}} = \pm\sqrt[3]{\frac{x_s}{8t}} \\ &\Rightarrow x\left(x_0^{\pm}(t)\right) = x_0^{\pm}(t) + t\,u_0\left(x_0^{\pm}(t)\right) = \pm x_s(t). \end{aligned} \tag{6.7}$$

and the solution is

$$U(x,t) = \begin{cases} (8t)^{-1/3}\left\{\sqrt[3]{x + \sqrt{x^2 - x_s^2}} + \sqrt[3]{x - \sqrt{x^2 - x_s^2}}\right\} & t \neq t_* \\ \sqrt[3]{\frac{x}{4t_*}} & t = t_* \end{cases} \tag{6.8}$$

Note the particular (real) values of $u(x,t)$ on both sides of the shock at $x = 0^{\pm}$:

$$u(0^{\pm},t) = -U(0^{\pm},t)/t = \begin{cases} \mp\frac{1}{2}(t - t_*)^{1/2}t^{-3/2}t_*^{-1/2} & t \geqslant t_* \\ 0 & t < t_* \end{cases} \tag{6.9}$$

The topology of the three-sheeted Riemann surface given by (6.8) and the interpretation of the shock as the permutation of two Riemann sheets has been fully explained by Bessis and Fournier in [5].

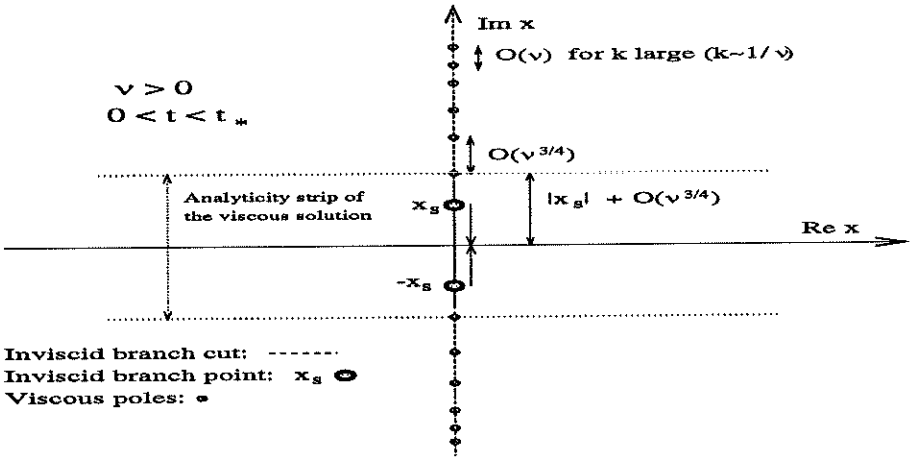

FIG. 6.2. *Inviscid branch points, branch cuts and viscous poles for $\nu > 0$ and $0 < t < t_*$. The poles are located above the inviscid branch point singularities according to the asymptotic formula $\beta_k(t,\nu) = \Im x_s(t) + \mathcal{O}\left((k\nu)^{3/4}\right)$. Moreover the distance separating two succesive poles is asymptotically given by $\Delta\beta_k = \mathcal{O}(\nu)$ as $\nu \to 0^+$ for k large ($k \sim 1/\nu$).*

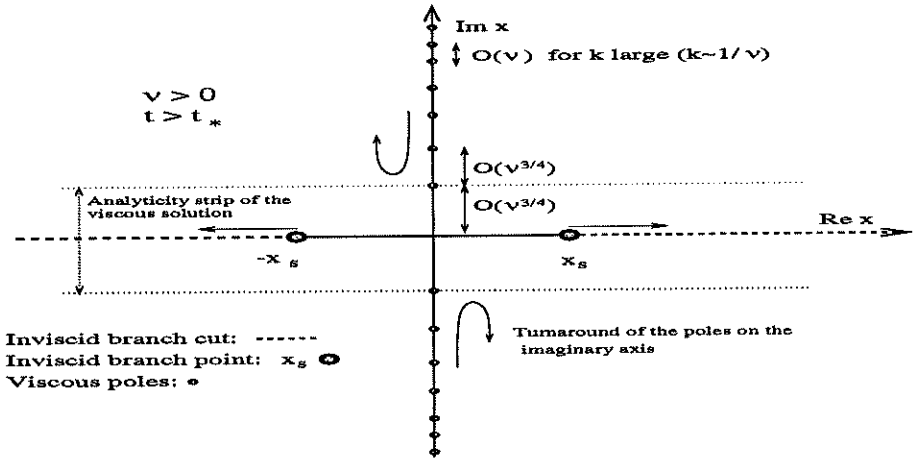

FIG. 6.3. *Inviscid branch points, branch cuts and viscous poles for $\nu > 0$ and $t > t_*$. The inviscid branch points have coalesced at $t = t_*$ at the origin, and are now moving away from each other on the real axis. However the poles are fixed to the imaginary axis and are asymptotically given by $\beta_k(t,\nu) = \mathcal{O}\left((k\nu)^{3/4}\right)$ as $\nu \to 0^+$, and $\Delta\beta_k = \mathcal{O}(\nu)$ as $\nu \to 0^+$ for k large ($k \sim 1/\nu$). They turn around and move away from the origin at a time $t_u > t_*$ if ν is small enough (if $\nu \gtrapprox .01$, $t_u < t_*$).*

A. On the generic nature of the initial data. Caflisch *et altri* characterize geometrically generic singularities for nonlinear hyperbolic systems in [10] in the following way: given a PDE and its initial data, a singularity is generic if, under perturbation of the "initial data", the singularity is of one of the stable types, namely a fold corresponding to a square-root branch point in z for each t, or a cusp corresponding to a cube root branch point which occurs when the two square root branch-points collide. They show that these are the only stable singularity types for the inviscid Burgers' equation. Loosely, they define stability as the property that under perturbation of the initial data, the perturbed solution will have the same singularity type as the original problem, i.e. either a a fold or a cusp. Note that the formation of a cube root singularity must stem from a "tangential" collision of the square root branch

points, i.e. one where the branch points travel at the same characteristic speed. In case of a "non-tangential" collision of square root branch points travelling at different characteristic speeds, the resulting singularity remains a square root branch point. For more details see [10].

Fournier and Frisch characterized generic singularities and corresponding generic initial data for the inviscid Burgers' equation in [17]. This description is based on a local analysis of the singularity and takes into account the Gallilean invariance of the PDE, and its invariance under translation of the reference frame. This was reformulated in Bessis and Fournier's first paper [6]. For the reader's convenience we will recall this analysis: the shock time t_* at which the velocity $u(x,t)$ has an infinite gradient is given by $t_* = -(\inf_{x_0} u_0'(x_0))^{-1}$, after setting $1+tu_0'(x_0) = 0$. This condition arises from the invertibility of equation (6.3). Geometrically it reflects the crossing of two characteristics in the (x,t) plane. Let x_{0*} be the point in space where the gradient of the velocity field first reaches its lowest bound, and x_* its corresponding Eulerian coordinate:

$$\begin{cases} \inf_{x_0} u_0'(x_0) = u_0'(x_{0*}) \\ x_*(t) = x_{0*} + tu_0(x_{0*}). \end{cases}$$

It is then easy to see that

$$\frac{\partial u}{\partial x}(x_*(t),t) = \frac{\partial u}{\partial x_0}(x_{0*},t) \Big/ \frac{\partial x}{\partial x_0}(x_*) = \frac{u_0'(x_{0*})}{1+tu_0'(x_{0*})} \xrightarrow{t \to t_*} \infty$$

One can place the shock at the origin ($x_{0*} = 0$) by coordinate translation $x \to x - x_{0*}$, and we can also set $u_0(x_{0*}) = u_0(0) = 0$ by virtue of the Gallilean invariance of the PDE. Indeed, setting $u \to u - c$, $x \to x + ct$ leaves the PDE unchanged. We also set $u_0''(0) = 0$ in order to have an inflexion point where the velocity field has an infinite gradient at $t = t_*$. $u_0(x_0)$ therefore has the form

$$u_0(x_0) = -\frac{x_0}{t_*} + bx_0^3 + \mathcal{O}(x_0^4).$$

The Eulerian coordinate x is locally given by

$$x(x_0,t) = \left(1 - \frac{t}{t_*}\right) x_0 + btx_0^3 + \mathcal{O}(x_0^4).$$

The Lagrangian coordinate x_0 is correspondingly

$$x_0(x,t) = \begin{cases} \dfrac{x}{1-t/t_*} + \mathcal{O}(x^3) & 0 < t < t_* \\ \sqrt[3]{\frac{x}{bt_*}} + \mathcal{O}(x^{2/3}) & t = t_* \end{cases}$$

In a neighborhood of the origin, the solution is locally given by

$$u(x,t) = \begin{cases} \dfrac{x}{t-t_*} + \mathcal{O}(x^3) & 0 < t < t_* \\ -\sqrt[3]{\frac{x}{bt_*^4}} + \mathcal{O}(x^{2/3}) & t = t_* \end{cases}$$

This analysis clearly shows the formation of the cube-root singularity at the shock time t_* (for more details see [6, 17]).

B. Cardan's formula. The roots of a cubic polynomial are given by the well known formula of Cardan (cf. [2, §3.8.2]). We state this formula to clarify the choices that are made in choosing the branches of the algebraic functions which define the saddle points in the expansions: Let $\lambda,a,b,c \in \mathbb{C}$, then the roots of the equation

$$\lambda^3 + a\lambda^2 + b\lambda + c = 0 \tag{B.1}$$

are obtained by setting

$$A = a/3, \quad B = b/3, \quad \alpha = A^2 - B, \quad \zeta = 2A^3 - 3AB + c.$$

Let $\lambda = x - A$, then (B.1) becomes

$$x^3 - 3\alpha x + \zeta = 0 \tag{B.2}$$

Let $\omega = e^{2\pi i/3}$ be a cube root of unity, then the three roots of (B.2) are:

$$\text{(B.3)} \qquad \begin{cases} x_0 = \omega\mathcal{A} + \omega^2\mathcal{B} \\ x_1 = \omega^2\mathcal{A} + \omega\mathcal{B} \\ x_2 = \mathcal{A} + \mathcal{B} \end{cases} \quad \text{where} \quad \begin{cases} \Delta = \left(\frac{\zeta}{2}\right)^2 - \alpha^3 \\ \mathcal{A} = \sqrt[3]{-\frac{\zeta}{2} + \sqrt{\Delta}} \\ \mathcal{B} = \sqrt[3]{-\frac{\zeta}{2} - \sqrt{\Delta}} \end{cases}$$

After choosing a branch for $\mathcal{A}$, one must choose the corresponding branch for $\mathcal{B}$ so that $\mathcal{A}\cdot\mathcal{B} = \alpha^3$. If α and ζ are real, then there are three possibilities depending on the sign of the real discriminant Δ:

(i) $\underline{\Delta < 0}$	(ii) $\underline{\Delta = 0}$	(iii) $\underline{\Delta > 0}$
$\mathcal{A},\mathcal{B} \in \mathbb{C},\ \mathcal{A} = \overline{\mathcal{B}}$	$\mathcal{A} = \mathcal{B} \in \mathbb{R}$	$\mathcal{A},\mathcal{B} \in \mathbb{R}$
$x_0, x_1, x_2 \in \mathbb{R}$	$x_0 = x_1 = -\frac{x_2}{2} \in \mathbb{R}$	$x_0 = \overline{x_1} \in \mathbb{C},\ x_2 \in \mathbb{R}$

When $\nu > 0$ (see § 4.2), case (iii) which yields two conjugate roots is the only instance when we can expect to have two equally relevant saddle points, thus allowing for some cancellation in the asymptotic expansion. The relevant roots x_0 and x_1, after separation of real and imaginary parts, are given by

$$x_0 = \overline{x_1} = -\frac{1}{2}(\mathcal{A} + \mathcal{B}) + i\frac{\sqrt{3}}{2}(\mathcal{A} - \mathcal{B}). \tag{B.4}$$

Acknowledgment. The author expresses his gratitude to Prof. R. Caflisch for introducing him to this subject, for his help, continuing support and interest which made this work possible. The author would also like to thank Prof. D. Bessis, Prof. N. Ercolani, Prof. J.D. Fournier, and Dr. C. Rippel for many valuable conversations. Special thanks to Prof. L. Greengard for the expeditious use of his Multipole code which greatly enhanced the numerical pole dynamics. The author is also deeply indebted to Dr. D. Petrasek and Dr. H. Rahimizadeh for their help and encouragement, and Prof. K. Holczer for his encouragement, hospitality and helpful discussions.

REFERENCES

[1] M.J. Ablowitz and H. Segur, *Solitons and the Inverse Scattering Transform*, Siam, 1981, pp. 203-209.

[2] M. Abramowitz and I.A. Stegun, *Handbook of Mathematical Functions*, Dover, 1965.

[3] L.V. AHLFORS, *Complex Analysis*, Mc.Graw Hill, 3rd. edition, 1979.
[4] C. BARDOS AND S. BENACHOUR, *Domaine d'analyticité des solutions de l'équation d'Euler dans un ouvert de* $\mathbb{R}^n$, Annali della Scuola Normale Superiore di Pisa, IV,4 (1977), pp. 647-687.
[5] D. BESSIS AND J.D. FOURNIER, *Complex singularities and the Riemann surface for the Burgers equation*, Research Reports in Physics - Nonlinear Physics, Springer Verlag Berlin, Heidelberg 1990, pp. 252-257.
[6] D. BESSIS AND J.D. FOURNIER, *Pole condensation and the Riemann surface associated with a shock in Burgers equation*, J.Phys.Lett. **45** (1984), L833-L841.
[7] R.P. BOAS, *Entire Functions*, Academic Press Inc., 1954.
[8] J.M. BURGERS, *The Nonlinear Diffusion Equation*, D. Reidel Publishing Co., 1974.
[9] J.M. BURGERS, *A mathematical model illustrating the theory of turbulence*, Adv. Appl. Mech., Vol 1 (1948), pp. 171-199.
[10] R.E. CAFLISCH, N. ERCOLANI, T.Y. HOU AND Y. LANDIS, *Multi-valued solutions and branch point singularities for nonlinear hyperbolic or elliptic systems*, Comm. Pure Appl. Math. **46** (1993), pp. 453-499.
[11] F. CALOGERO, *Motion of poles and zeros of special solutions of nonlinear and linear partial differential equations and related "solvable" many body problems*, Il Nuovo Cimento **43B** No. 2 (1978), pp. 177-241.
[12] J. CARRIER, L. GREENGARD AND V. ROKHLIN, *A fast adaptive multipole algorithm for particle simulations*, SIAM J. Sci. and Stat. Comp. **9** (1988), pp. 669-686.
[13] C. CHESTER, B. FRIEDMAN AND F. URSELL, *An extension of the method of steepest descents*, Proc. Camb. Phil. Soc. **53** (1957), pp. 599-611.
[14] D.V. CHOODNOVSKY AND G.V. CHOODNOVSKY, *Pole expansions of nonlinear partial differential equations*, Il Nuovo Cimento **40B** No. 2 (1977), pp. 339-353.
[15] J.D. COLE, *On a quasi-linear parabolic equation occuring in aerodynamics*, Quart. Appl. Math. **9** (1951), pp. 225-236.
[16] A.R. FORSYTH, *Theory of Differential Equations*, Part IV, Vol. **6**, Dover, 1906.
[17] J.D. FOURNIER AND U. FRISCH, *L'équation de Burgers deterministe et statistique*, J. Mec. Th. Appl. **2** (1983), pp. 699-750.
[18] U. FRISCH AND R. MORF, *Intermittency in nonlinear dynamics and singularitites at complex times*, Phys. Rev. A **23**, No. 5 (1981), pp. 2673-2705.
[19] L. GREENGARD AND V. ROKHLIN, *A fast algorithm for particle simulations*, J. Comp. Phys. **73** (1987), pp. 325-348.
[20] E. HOPF, *The partial differential equation* $u_t + u\,u_x = \mu\,u_{xx}$, Comm. Pure Appl. Math. **3** (1950), pp. 201-230.
[21] D. KAMINSKI, *Asymptotic expansion of the Pearcey integral near the caustic*, SIAM J. Math. Anal., **20** (1989), pp. 987-1005.
[22] Y. KIMURA, *Dynamics of complex singularities for Burgers' equation*, Proc. NEEDS '94, edited by V.G. Makhankov, World Scientific, Singapore, 1995.
[23] R.B. PARIS, *The asymptotic behavior of Pearcey's integral for complex variables*, Proc. Roy. Soc. London, Ser. A **432** (1991), pp. 391-426.
[24] G. PÓLYA, *Über trigonometrische integrale mit nur reellen nullstellen*, Journal für die reine und angewandte Mathematik **158** (1927), pp. 6-18.
[25] D. SENOUF, *Asymptotic and numerical approximations of the zeros of Fourier integrals*, to appear in SIAM J. Math. Anal.
[26] D. SENOUF, *On the zero-viscosity limit of Burgers' equation from the perspective of complex singularities*, submitted to SIAM J. Math. Anal.
[27] D. SENOUF, *Complex singularities for Burgers' equation with complex viscosity and asymptotic approximations of the zeros of Fourier integrals*, Ph.D. Dissertation, UCLA (1994).
[28] D. SENOUF, R. CAFLISCH AND N. ERCOLANI, *Dynamics of complex singularities for Schrödinger's equation with convective nonlinearity in the small dispersion limit*, in progress.
[29] C. SULEM, P.L. SULEM, AND H. FRISCH, *Tracing complex singularities with spectral methods*, J. Comp. Phys. **50** (1983), pp. 138-161.
[30] O. THUAL, U. FRISCH AND M. HÉNON, *Application of pole decomposition to an equation governing the dynamics of wrinkled flame fronts*, J. Phys. **46** (1985), pp. 1485-1494.
[31] F. URSELL, *Integrals with a large parameter. Several nearly coincident saddle points*, Proc. Cambridge Phil. Soc., **72** (1972), pp. 49-65.
[32] G.B. WHITHAM, *Linear and Nonlinear Waves*, Wiley Interscience, 1974.
[33] R. WONG, *Asymptotic Approximations of Integrals*, Academic Press, 1989.